

# The potential use of crushed waste glass as a sustainable alternative to natural and manufactured sand in geotechnical applications

Danish Kazmi <sup>a</sup>; Mehdi Serati <sup>a</sup>; David J. Williams <sup>a</sup>; Sadaf Qasim <sup>b</sup>; Yi Pik Cheng <sup>c</sup>

<sup>a</sup> Geotechnical Engineering Centre, School of Civil Engineering, The University of Queensland, Brisbane, QLD, 4072, Australia

<sup>b</sup> Department of Civil Engineering, NED University of Engineering and Technology, Karachi, 75270, Pakistan

<sup>c</sup> Department of Civil, Environmental and Geomatic Engineering, University College London, London, WC1E 6BT, United Kingdom

## Abstract

The increasing price and diminishing reserves of construction sand encourage a need to develop its sustainable and cost-effective replacement, helping the transition towards a circular economy. Waste glass is a derivative of natural sand and could potentially show similar geotechnical behaviour. Using crushed waste glass (CWG) as an alternative to traditional sand would potentially offer a double-duty benefit by helping to address the geo-environmental challenges of natural sand depletion and disposal of ever-increasing waste glass, together. This study investigated the geotechnical, mineralogical and morphological behaviour of CWG and compared it with that of natural sand (NS) and manufactured sand (MS). The geotechnical characterisation results showed that the behaviour of CWG is similar to the other two sands studied, with CWG showing the highest permeability and abrasion resistance. Surprisingly, the shear strength testing showed that the friction angle of CWG was higher under saturated conditions than under dry conditions, indicating the stability of CWG under saturated conditions. The mineralogical analysis was conducted using x-ray fluorescence (XRF) spectroscopy and revealed that silica is the dominant mineral in all three materials, indicating a similarity in their chemical composition. The morphological analysis was performed to quantify the particle shape of each material in terms of roundness index using digital images obtained through an optical microscope. The results demonstrated that MS showed the highest particle angularity, followed by CWG and NS. Overall, it was concluded that CWG could potentially act as a next-generation alternative and smart geomaterial, replacing traditional sands in several geotechnical applications.

## Keywords

Construction sand; circular economy; crushed waste glass; x-ray fluorescence (XRF) spectroscopy; optical microscope; smart geomaterial

## List of abbreviations

NS	Natural sand
MS	Manufactured sand
CWG	Crushed waste glass
XRF spectroscopy	X-ray fluorescence spectroscopy
LVDT	Linear variable differential transformer
OM	Optical microscopy
CLT	Central limit theorem
NSE	Nash-Sutcliffe model efficiency coefficient
SF	Normalised shape factor

## 44 1. Introduction

45 Natural aggregates are widely used in a range of applications. Presently, the construction  
46 industry is the biggest consumer of natural resources in the world (Bogas et al., 2015). It is a  
47 common practice to crush and screen the rock formations to different specifications, producing  
48 aggregates suitable for different construction applications (Xu et al., 2018a). The global  
49 consumption of aggregates is expected to increase at a rate of 5% per annum (Dhir et al., 2019).  
50 Major sources of natural construction aggregates include crushed stone, gravel, and sand  
51 (Kelly, 1998). In Australia alone, nearly 130 million tonnes of aggregates are extracted each  
52 year, which is expected to further increase in the coming years (Cement Concrete and  
53 Aggregates Australia, 2011). A key concern for sustainable infrastructure construction is the  
54 continuous diminution of readily-available construction aggregates (Holmstrom & Swan,  
55 1999). Environmentally, the extraction and logistics of aggregates release carbon footprint,  
56 which is harmful to the ecosystem (Bravo et al., 2015). Consequently, nowadays, construction  
57 materials are increasingly being evaluated by their ecological footprint (Hebhoub et al., 2011).

58 Natural sand is a widely used raw material and has become the second-most widely consumed  
59 natural resource on planet Earth, after freshwater (WACA, 2018). It is estimated that between  
60 32 and 50 billion tonnes of sand and gravel are extracted globally each year, which is largely  
61 used in construction (Koehnken & Rintoul, 2018). As an example, the construction of a  
62 medium-sized house requires 200 tonnes of sand; a hospital needs 3000 tonnes of sand, and  
63 each kilometre of highway construction needs 30,000 tonnes of sand (WACA, 2018). Studies  
64 show that sand is currently being extracted at a rate far greater than its renewal (Peduzzi, 2014).  
65 Indiscriminate mining of sand could endanger animal species and habitats, harm aquatic life  
66 and cause biodiversity loss (Koehnken et al., 2020). It could also cause beach erosion, making  
67 coastal communities vulnerable to floods and causing loss to the eco-tourism industry (Jonah  
68 et al., 2015). It is, therefore, necessary to find ways to reduce the demand for natural sand and  
69 to look for sustainable and low-carbon alternatives.

70 One of the ways of reducing the consumption of natural sand is to utilise wastes as an  
71 alternative material (Emery, 1974). Recycling of wastes could reduce the demand for virgin  
72 natural resources and help to dispose of them effectively (Kazmi et al., 2019b). The volumes  
73 of wastes generated each year are alarmingly increasing due to a rise in the global population.  
74 The world produces nearly 2.0 billion tonnes of municipal solid waste every year, which is  
75 expected to grow to 3.4 billion tonnes by 2050 (Kaza et al. 2018). In Australia, nearly  
76 67 million tonnes of waste was produced in 2016-17, equivalent to 2.7 tonnes per capita per  
77 year (Pickin et al., 2018). Statistics show that around 40% of waste is landfilled each year in  
78 Australia (Department of the Environment and Energy, 2013). It is imperative to minimise the  
79 amount of solid waste landfilled every year to promote environmental sustainability, waste  
80 valorisation and to minimise resource consumption (Vining et al., 1992). Typically, recycling  
81 is regarded as an eco-friendly strategy for solid waste management that is superior to landfilling  
82 or incineration (Peng et al., 1997). Besides the conservation of energy and materials, recycling  
83 typically decreases the need for landfilling and incineration, reduces pollution, and contributes  
84 positively to the environment (Woodford, 2019).

85 Waste glass, sometimes also called cullet, is commonly found in mixed waste. Statistics show  
86 that volumes of waste glass generated every year are constantly increasing. In 2016, the waste  
87 glass accounted for 5% of the total waste generated globally (Kaza et al. 2018). In Australia  
88 alone, nearly 1.1 million tonnes of waste glass was produced in 2016-17, with 43% remaining  
89 unrecycled. The stockpiles of waste glass are continuously increasing, creating a disposal  
90 challenge (Arulrajah et al., 2012b). According to the European Union (EU) statistical data,  
91 glass is the third most common packing material. In 2017, the EU generated nearly 173.8 kg

92 of packaging waste per capita, comprising a huge 18% glass (Eurostat, 2020). Although  
93 colourless glass could be used for glass re-manufacturing, the multi-coloured waste glass is  
94 often sent for landfilling (Park & Lee, 2004). A key reason limiting the use of waste glass for  
95 glass-remanufacturing is the expensive colour sorting of waste glass fragments necessary to  
96 avoid colour contamination, making its use often uneconomical in glass re-manufacturing due  
97 to a substantial increase in the cost of furnace-ready cullet (Amiri et al., 2018). Moreover, the  
98 colour sorting of waste glass is sometimes impractical, because a large volume of waste glass  
99 supplied to the recycling industry is broken into smaller fragments during the logistics, making  
100 it difficult to colour sort waste glass due to its smaller particle size (Arulrajah et al., 2015).

101 Glass is relatively inert and could take several hundred years to biodegrade (Salamatpoor &  
102 Salamatpoor, 2017). Waste glass not only consumes precious landfill space, but it also causes  
103 environmental pollution (Jani & Hogland (2014); making landfilling of waste glass an  
104 environmentally unsustainable solution (Rashad, 2014). The increasing scarcity of landfill  
105 spaces necessitates the development of new and self-sustaining applications of waste glass,  
106 together with finding ways to promote its recycling. Greater recycling of waste glass would  
107 reduce pressure on landfills and promote the circular economy, an economic model wherein  
108 planning, resourcing, procurement, production and reprocessing are designed and managed to  
109 maximise human well-being and ecosystem functioning (Murray et al., 2017). This model has  
110 been proposed as an alternative to the traditional linear-extract-produce-use-dump material and  
111 energy flow model, which is increasingly unsustainable (Frosch & Gallopoulos, 1989). The  
112 circular economy model promotes minimising wastes by utilising them as an input for other  
113 applications, thereby promoting recycling (Stahel, 2016).

114 Crushed waste glass (CWG) has been studied for use in various secondary applications. For  
115 example, CWG has been studied as a fluxing agent for decreasing the firing temperature  
116 required in ceramic production (Shishkin et al., 2020). Similarly, Shishkin et al. (2019)  
117 investigated CWG as an additive for the production of clay-glass aggregate for building  
118 construction. Marangoni et al. (2014) analysed the use of CWG for the production of glass-  
119 ceramic foams. Chen et al. (2020) explored the fire resistance performance of cementitious  
120 composites containing CWG. Several studies have shown that CWG may be partially used as  
121 supplementary cementitious material and alternative to fine-grained aggregates in concrete  
122 production (Kazmi et al., 2019b). These applications, among others, typically utilise only some  
123 of the CWG produced (generally less than 40%). Limited geotechnical engineering studies  
124 have shown that CWG could potentially be used as a backfilling material in embankments,  
125 drainage blankets and road pavements. However, the use of CWG could be extended to other  
126 geotechnical applications, such as granular piles, which could potentially consume a much  
127 greater amount of CWG, possibly fully replacing traditional sand with CWG. Moreover, due  
128 to the absence of cementitious material containing alkali, several geotechnical applications,  
129 such as granular piles, could potentially utilise multi-coloured glass as an alternative to  
130 traditional aggregates, which could help divert waste glass from landfills.

131 One of the ways to recycling waste glass is to use it as a sustainable alternative to diminishing  
132 and increasingly expensive natural sand. Both sand and waste glass have a similar chemical  
133 composition and contain silica as a primary mineral. Typically, waste glass has angular  
134 particles and exhibits geotechnical parameters similar to natural aggregates (Arulrajah et al.,  
135 2012a). Using CWG as a replacement for natural sand could potentially offer two-pronged  
136 environmental and economic benefits, including a decrease in greenhouse gas emissions due  
137 to quarrying activities, reduction in an ever-increasing demand for natural sand, conservation  
138 of virgin sand reserves, reduced travelling time and distance of sand, and greater cost-

139 effectiveness (Kazmi et al., 2019a). Simultaneously, it would potentially have a knock-on  
140 effect of providing socio-economic benefits, promoting sustainable resource recovery,  
141 reducing landfill burden and developing a sustainable supply chain of waste glass. Presently, a  
142 lack of knowledge on the geotechnical behaviour of CWG is the biggest barrier in its use in  
143 geotechnical projects (Disfani et al., 2011b). In civil engineering, previous literature shows that  
144 the use of CWG has been mostly studied in concrete as an alternative to fine-aggregates and as  
145 supplementary cementitious material (Jani & Hogland, 2014). However, the studies exploring  
146 the geotechnical potential of CWG are relatively limited, mainly involving its use in road  
147 pavements and as soil additive; potentially due to a knowledge gap on the geo-environmental  
148 behaviour of CWG (Disfani et al., 2011a). This research aims to develop new geotechnical  
149 applications of CWG as an alternative geomaterial by comparing its behaviour with traditional  
150 sands.

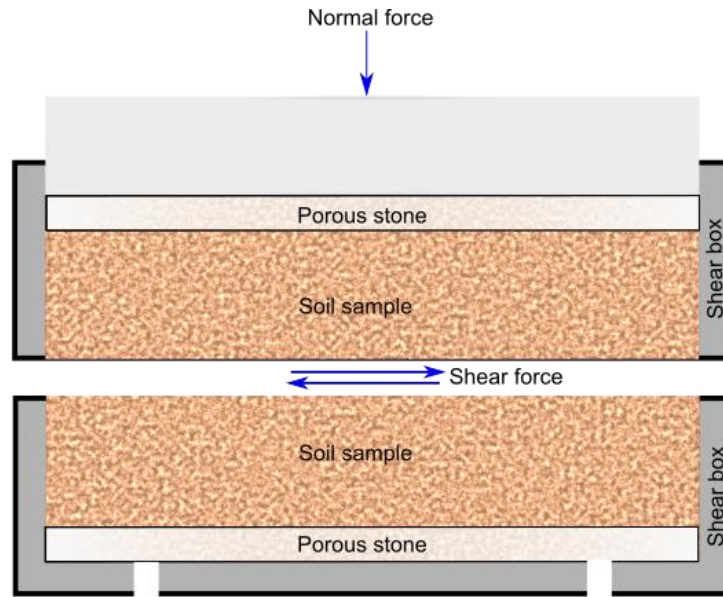
## 151 **2. Materials and Methodology**

152 Motivated by the above observations, this study compared the geotechnical potential of CWG  
153 with that of traditionally-used natural sand (NS) and manufactured sand (MS), which comes  
154 from two major sources of construction sand, i.e. beach and quarry. NS and MS were obtained  
155 from the beach of Pine River and from Mount Coot-tha quarry respectively in Queensland,  
156 Australia. CWG was obtained from a commercial supplier, Enviro sand, in Brisbane, utilising  
157 100% recycled glass, and milling it using a mining crusher under near-dry conditions (less than  
158 2% moisture content).

159 The experimental program involves performing three different analyses, including  
160 geotechnical, mineralogical and morphological, on the three materials. A key motivation to  
161 conduct the mineralogical analysis was to determine the silica content, which is typically a  
162 primary mineral in both sand and glass. X-ray fluorescence (XRF) spectroscopy was used to  
163 perform the mineralogical analysis on the three samples, using a fused bead Li-borate technique  
164 with an energy-dispersive X-ray fluorescence spectrometer (ED-XRF), XEPOS HE, (Spectro,  
165 Germany). The *Spectro XEPOS HE* is a dual anode system with palladium (Pd) for high energy  
166 excitation and cobalt (Co) for low energy excitation. The accelerating voltage is increased over  
167 the range 6 to 19 keV (elements Co to U), but the elements with X-ray lines lower than 6 keV  
168 (lighter than Co) are less excited. The range between 3 keV and 6 keV (elements K to Fe)  
169 incorporates bandpass and polarising filters using the Co target. The region below 3 keV uses  
170 the L-spectral lines of the Pd target and a polarising target for increased sensitivity. The *Spectro*  
171 *ED-XRF* measures three energy ranges, which were optimised for the ranges of interest (i.e.  
172 <3 keV, 3 to 6 keV and 6 to 19 keV).

173 The geotechnical analysis initially involved characterisation testing, including the sieve  
174 analysis, hydraulic conductivity, specific gravity, densities, and abrasion loss. The specific  
175 gravity and hydraulic conductivity of the materials were determined using the Helium gas  
176 pycnometer and constant head permeability test, respectively.

177 Afterwards, shear strength testing was performed using a direct shear apparatus. According to  
178 Das (2009), the direct shear apparatus comprises a split metal box in which the sample is  
179 placed. Figure 1 shows the arrangement of the direct shear test. The normal force on the sample  
180 is applied vertically using dead weights. The shear force is applied by moving the top half of  
181 the shear box relative to the fixed bottom half, causing shearing of the sample at the interface  
182 between the two halves of the shear box. During the experiment, the change in sample thickness  
183 and shear displacement of the top half are recorded using dial gauges or linear variable  
184 differential transformers (LVDTs). The shear strength parameters of the sample are then  
185 interpreted from the test results (Xu et al., 2018).



186

187

**Fig.1.** Direct shear test arrangements (Adapted from Das (2009))

188

189

190

191

The direct shear testing involved preparing the oven-dried samples in a loose-dry condition with dimensions 60 x 60 x 32 mm. Seven normal stresses, 6.8, 13.6, 27.2, 54.5, 109.0, 218.0 and 436.0 kPa, were applied under dry and saturated conditions. The saturated condition refers to testing in a bath, which for a sandy material would achieve full saturation.

192

193

194

195

196

197

198

199

200

201

202

An important parameter used to evaluate the suitability of material in construction applications is abrasion resistance, which is the ability of a surface to withstand degradation due to friction or rubbing (Safiuddin & Scott, 2015). Technically, the resistance of aggregates to degradation is typically a combination of two phenomena, including abrasion, denoting loss in the surface angularity of aggregate, and breakage, which refers to the fracturing of particles (Mahmoud, 2007). In construction, the aggregates are typically required to be tough and abrasion-resistant to withstand degradation, crushing and disintegration during various activities (Wu et al., 1998). It is, therefore, essential to evaluate the resistance to degradation of any alternative geomaterial before considering its use in construction. The abrasion loss in CWG was compared to that of NS and MS. Micro-Deval apparatus was used to perform the abrasion testing.

203

204

205

206

207

208

Moreover, the morphological analysis was conducted using a digital imaging technique to determine the particle shape (angularity) of the three materials. An optical microscope, containing a digital colour camera Leica DFC295 with a pixel depth of 3.2 μm x 3.2 μm, was used to image the sample particles followed by the analysis of microscopic images using an image processing software *ImageJ*. The shape of sample particles was calculated in terms of roundness index ( $R_i$ ) using the following equation as proposed by Wadell (1932).

209

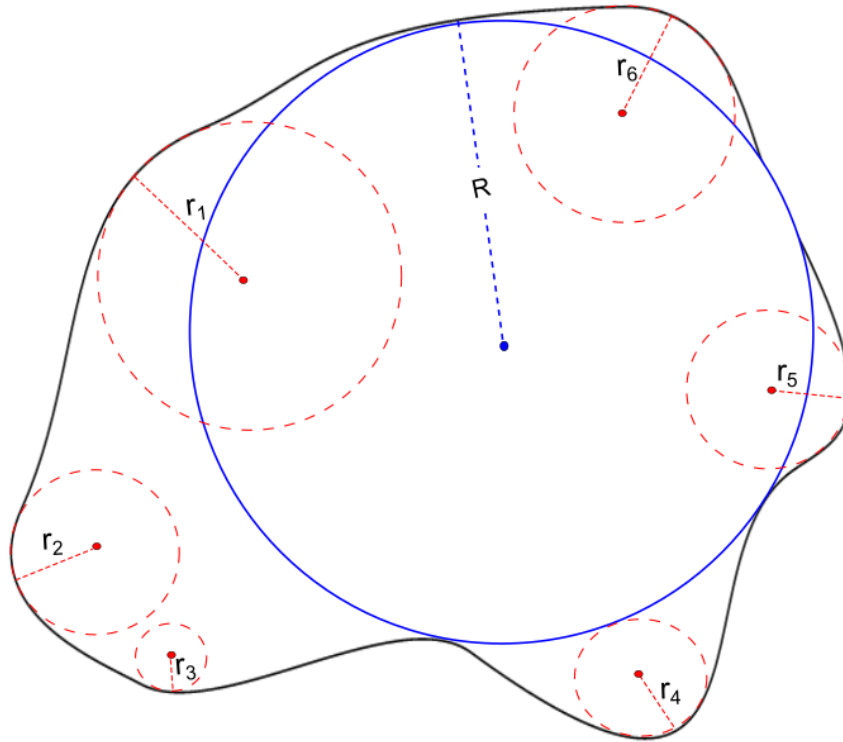
$$R_i = \frac{\sum_{i=1}^N r_i / N}{R} \quad (1)$$

210

211

212

Where,  $r_i$  is the radius of corners of the particle,  $N$  is the number of corners, and  $R$  is the radius of the largest inscribed circle. Figure 2 shows the graphical illustration to calculate the radii of the particle.



213

214

**Fig.2.** Graphical illustration for calculating the radii of a particle

215 The optical microscopy (OM) images were input into *ImageJ* software to calculate particle's  
 216 roundness index, which is the ratio of the mean radius of curvature of the corners of the  
 217 particle's silhouette to the radius of the largest inscribed circle. The particle roundness index  
 218 was determined using the method proposed by Wadell (1932). A roundness index value of 1  
 219 represents a perfectly round particle, whereas 0 represents an angular one. Overall, a total of  
 220 390 particles (i.e. grains) of each material were analysed for particle shape calculations.  
 221 Afterwards, the central limit theorem (CLT) was applied to estimate the mean roundness index  
 222 and to assess whether the particle roundness in each material has a normal distribution. The  
 223 results from the CLT can also be used to get an idea of the minimum number of particles  
 224 (grains) required to collect from each material for statistical analysis. According to CLT, given  
 225 a sufficiently large sample size (usually  $N > 30$ ) selected from a population with a finite variance  
 226 level, the mean of all sample sets drawn randomly from the population (with replacement) will  
 227 be equal to the population mean (i.e.  $\mu$ ), regardless of the population shape and distribution  
 228 (Ganti, 2019). That is, the sampling distribution of the sample means drawn from a population  
 229 with any distribution is approximately normally distributed with a mean ( $\mu_{\bar{x}}$ ) equals to the  
 230 population mean (i.e.  $\mu = \mu_{\bar{x}}$ ). It should be noted that if the original population (from which  
 231 the data is drawn) is normal itself, the sampling distribution of the sample means becomes  
 232 normally distributed even for small sample sizes (e.g.  $N > 5$ ). The standard deviation of the  
 233 sampling distribution of sample means ( $\sigma_{\bar{x}}$ ) is also related to the population's standard  
 234 deviation according to:

235

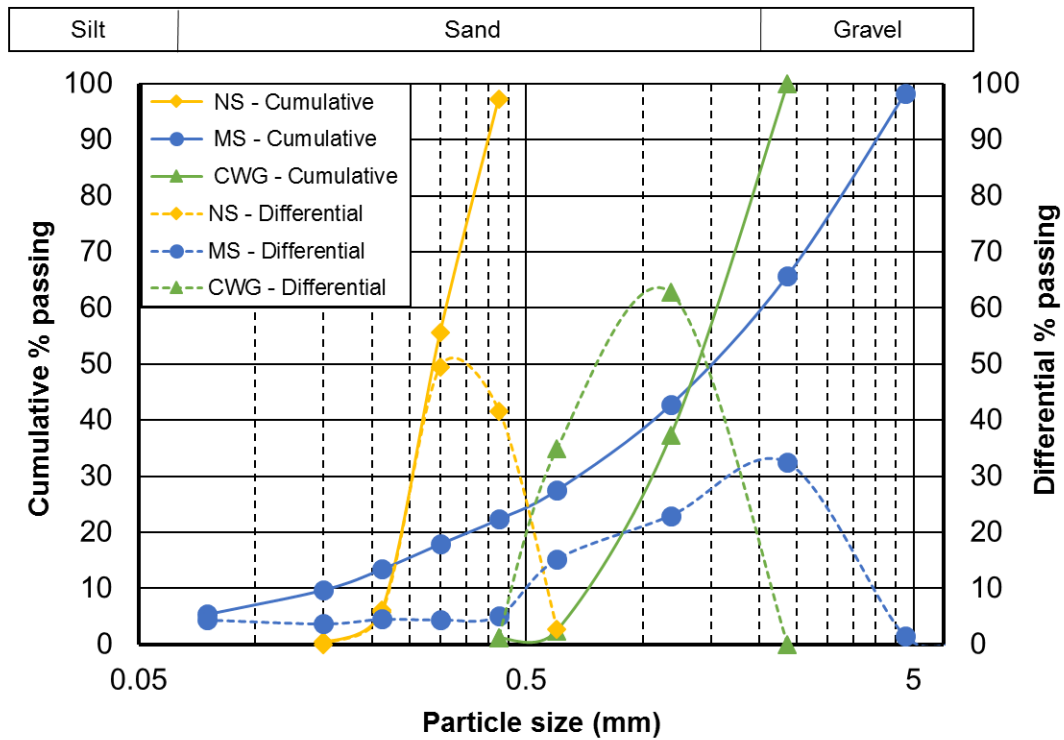
$$\sigma_{\bar{x}} = \frac{\sigma}{\sqrt{N}} \quad (2)$$

236 Where  $\sigma_{\bar{x}}$  and  $\sigma$  represents the standard deviation of the sampling distribution of sample means  
 237 and the population, respectively, with  $N$  representing the sample size. Different samples with  
 238 a size of 5, 10, 15, 20 and 25 particles were randomly selected from each material, and their  
 239 frequency distribution was plotted. Some manual adjustments were performed to ensure the  
 240 grains were clearly defined and did not overlap during imaging.

### 241 3. Geotechnical characterisation of materials

242 Figure 3 illustrates the gradation curves of the materials, while the gradation parameters are  
243 shown in Table 1. The results of sieve analysis showed that NS and CWG are uniformly graded  
244 materials, with a median grain diameter of 0.29 mm and 1.42 mm, respectively. The coefficient  
245 of uniformity ( $C_u = D_{60}/D_{10}$ ) and the coefficient of curvature ( $C_c = D_{30}^2/(D_{60} \times D_{10})$ ) for NS was  
246 found to be 1.43 and 0.94, respectively. Similarly, the coefficient of uniformity and curvature  
247 for CWG were found to be 2.21 and 0.96, respectively. Nevertheless, MS showed a well-graded  
248 gradation with a median grain diameter, coefficient of uniformity and coefficient of curvature  
249 of 1.55 mm, 13.37 and 1.51, respectively. The potential reason for a uniform gradation and  
250 smaller grain size of NS could be its process of deposition, governed primarily by wave action  
251 and ebb and flow of tides. For MS and CWG, the grain size and gradation are a function of  
252 several factors, such as the degree of crushing, sorting and sieving. Table 2 shows the  
253 geotechnical parameters of the materials. The specific gravity of all three materials was  
254 comparable to each other and ranging 2.50-2.74, with MS and CWG having the maximum and  
255 minimum specific gravity, respectively. The potential reason for similar specific gravity of NS,  
256 MS and CWG could be the presence of silica as a primary mineral, considering that glass is  
257 essentially a derivative of sand. Previous literature shows that the permeability of CWG could  
258 be particularly sensitive to the presence of contaminants, such as organic content and debris  
259 (Dhir et al., 2018). The results of permeability tests demonstrated that CWG had the highest  
260 hydraulic conductivity, followed by NS and MS. The higher permeability of CWG could  
261 potentially be attributed to its uniform gradation and larger effective diameter ( $D_{10}$ ), causing a  
262 relatively higher maximum void ratio; noting that permeability of sands is directly proportional  
263 to their effective diameter (Hazen, 1892). CWG typically offers superior permeability  
264 characteristics, indicating its potential to act as a drainage media in various geotechnical  
265 applications (Disfani et al., 2011b).

266 The results of abrasion testing showed that CWG, surprisingly, outperformed NS and MS. It  
267 was observed that abrasion loss in CWG was nearly two and four times less than that of NS  
268 and MS, respectively (see Table 2); favouring the prospects of using CWG as an alternative  
269 geomaterial in traditional geotechnical applications.



270

**Fig.3.** Gradation curves of the materials

271

**Table 1.** Gradation parameters of the materials

	<b>NS</b>	<b>MS</b>	<b>CWG</b>
$C_u$	1.43	13.37	2.21
$C_c$	0.94	1.51	0.96
$D_{60}$ (mm)	0.31	2.07	1.61
$D_{50}$ (mm)	0.29	1.55	1.42
$D_{30}$ (mm)	0.25	0.69	1.06
$D_{10}$ (mm)	0.22	0.15	0.73

272

**Table 2.** Geotechnical parameters of the materials

	<b>NS</b>	<b>MS</b>	<b>CWG</b>	<b>Standard</b>
Minimum void ratio	0.59	0.39	0.37	-
Maximum void ratio	0.70	0.62	0.79	-
Gravimetric moisture content (%)	3.08	0.33	0.00	AS 1289.2.1.1-2005
Specific gravity	2.63	2.74	2.50	ASTM D5550 -14
Liquid limit (%)	22.72	19.33	-	AS 1289.3.9.1:2015
Minimum dry density ( $\text{g/cm}^3$ )	1.54	1.69	1.39	AS 1289.5.5.1-1998
Maximum dry density ( $\text{g/cm}^3$ )	1.65	1.96	1.82	AS 1289.5.5.1-1998
Hydraulic conductivity (m/s)	$3.81 \times 10^{-4}$	$3.59 \times 10^{-4}$	$4.01 \times 10^{-4}$	ASTM D2434-68
Abrasion loss (%)	6.00	9.60	2.40	ASTM D7428



273 **4. Experimental Results**

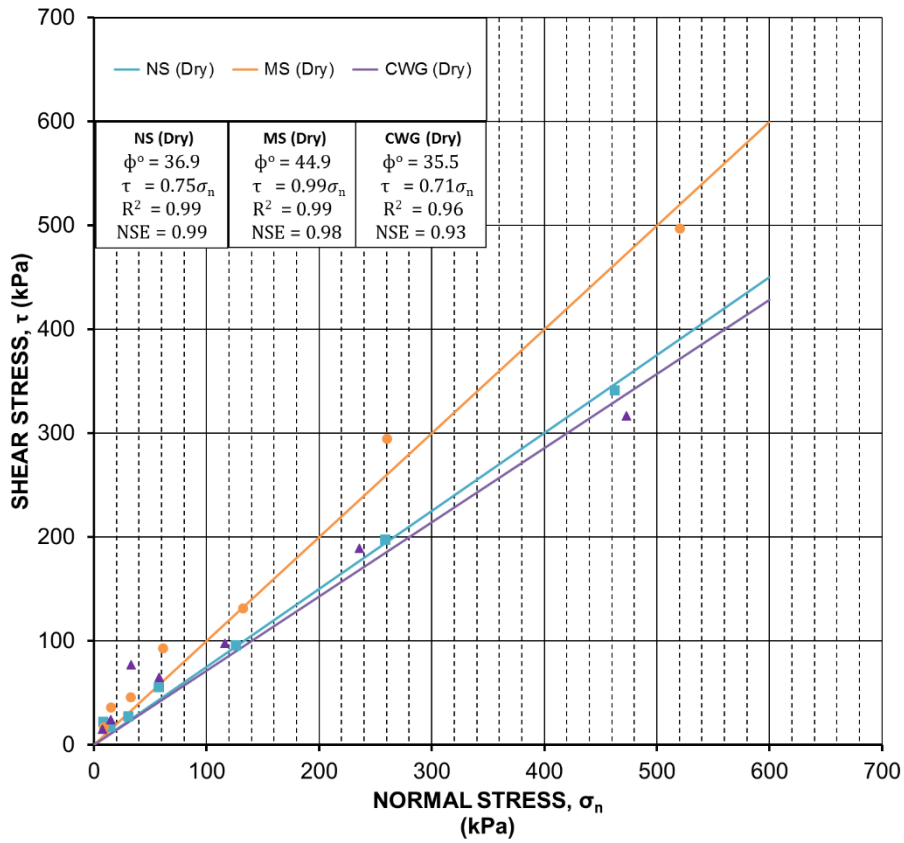
274 **4.1 Direct shear tests to determine the friction angles**

275 Oven-dried materials were used to prepare the direct shear samples in loose conditions. These  
 276 samples were subjected to direct shear testing at a shearing rate of 1.0 mm/min. The measured  
 277 shear stresses and applied normal stresses were corrected for reductions in the shear area during  
 278 the shearing process (Xu et al., 2018b). The shear strength envelopes were best-fitted by  
 279 applying the Mohr-Coulomb failure criterion. The value of cohesion (c) was set to zero as  
 280 uncemented sand does not typically exhibit cohesion. The fitting parameters are shown for each  
 281 of the envelopes in terms of the coefficient of determination ( $R^2$ ) and the Nash-Sutcliffe model  
 282 efficiency coefficient (NSE). The NSE was proposed by Nash and Sutcliffe (1970) to provide  
 283 a goodness-of-fit-index relatively superior to the correlation coefficient. One advantage of the  
 284 NSE is that it can be applied to a range of model types (McCuen et al., 2006). Several  
 285 researchers have previously applied the NSE in geotechnical engineering research, showing  
 286 that the NSE provides a more reliable statistical estimate of the goodness-of-fit (Mishra et al.,  
 287 2017; Mishra et al., 2018). An NSE value of 1 represents an ideal agreement between the model  
 288 and observed values (Criss & Winston, 2008). Based on the NSE criteria proposed by Chiew  
 289 and McMahon (1993), the goodness-of-fit of all shear strength envelopes presented in this  
 290 study can be classified as “perfect” ( $NSE \geq 0.93$ ).

291 Table 3 compares the peak and final friction angles of materials under dry and saturated  
 292 conditions. Figure 4 and 5 show the peak shear strength envelopes of materials under dry and  
 293 saturated conditions, respectively. Figure 6 and 7 shows the final shear strength envelopes of  
 294 materials under dry and saturated conditions, respectively. The results indicated that the peak  
 295 friction angle of MS under dry conditions was found to be the highest, 44.9°, followed by that  
 296 of NS (36.9°) and CWG (35.5°). Potential reasons for a relatively higher friction angle of MS  
 297 include relatively well-graded gradation and larger particle size, contributing to a lower void  
 298 ratio and higher inter-particle contact points. The highest angularity (i.e. lowest roundness  
 299 index, as shown in Table 6) of the MS could be a reason. Previous studies have also endorsed  
 300 that sands exhibiting a relatively higher friction angle typically have coarser-grained particles,  
 301 well-graded gradation and angular shape (Bareither et al., 2008).

302 **Table 3.** Comparison of peak and final friction angles of the materials under dry and  
 303 saturated conditions

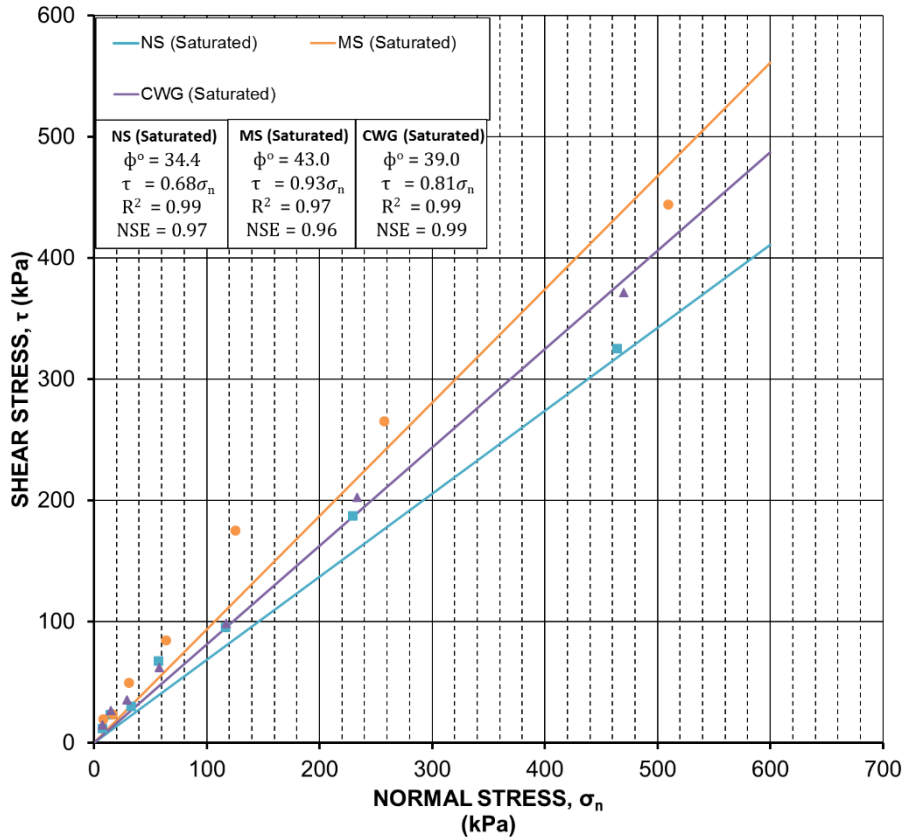
Angle of internal friction (°)	NS		MS		CWG	
	Peak					
	Dry	Saturated	Dry	Saturated	Dry	Saturated
	36.9	34.4	44.9	43.0	35.5	39.0
	Final					
31.1	30.7	44.1	41.3	29.1	32.4	



304

305

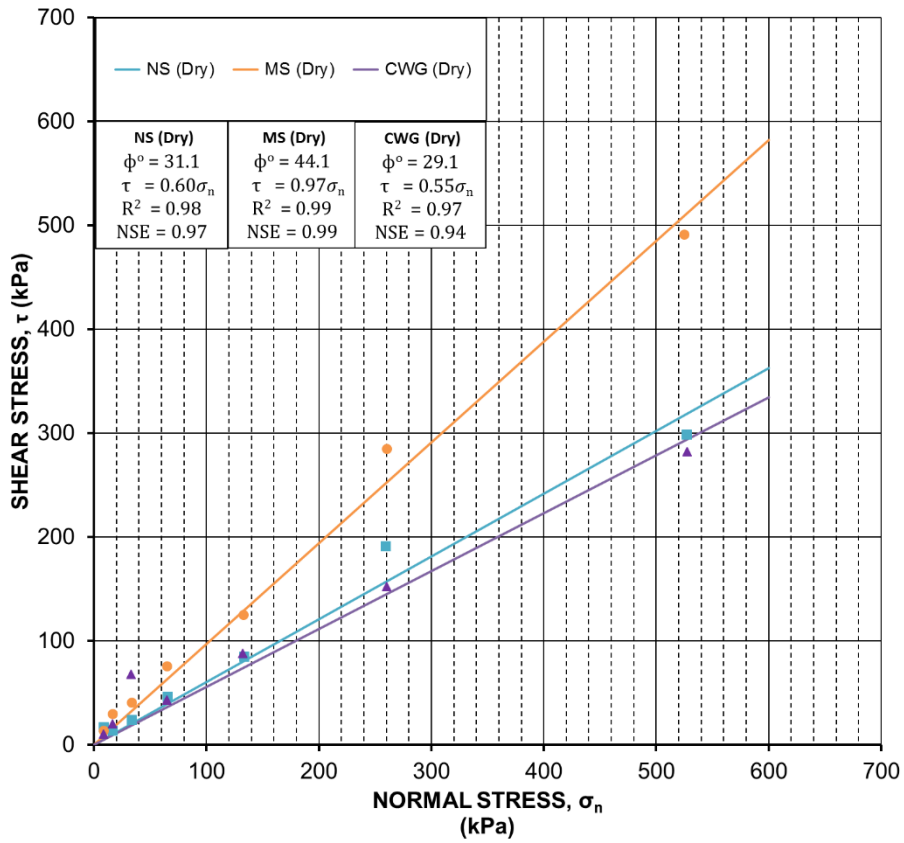
**Fig.4.** Peak shear strength envelopes of the materials under dry conditions



306

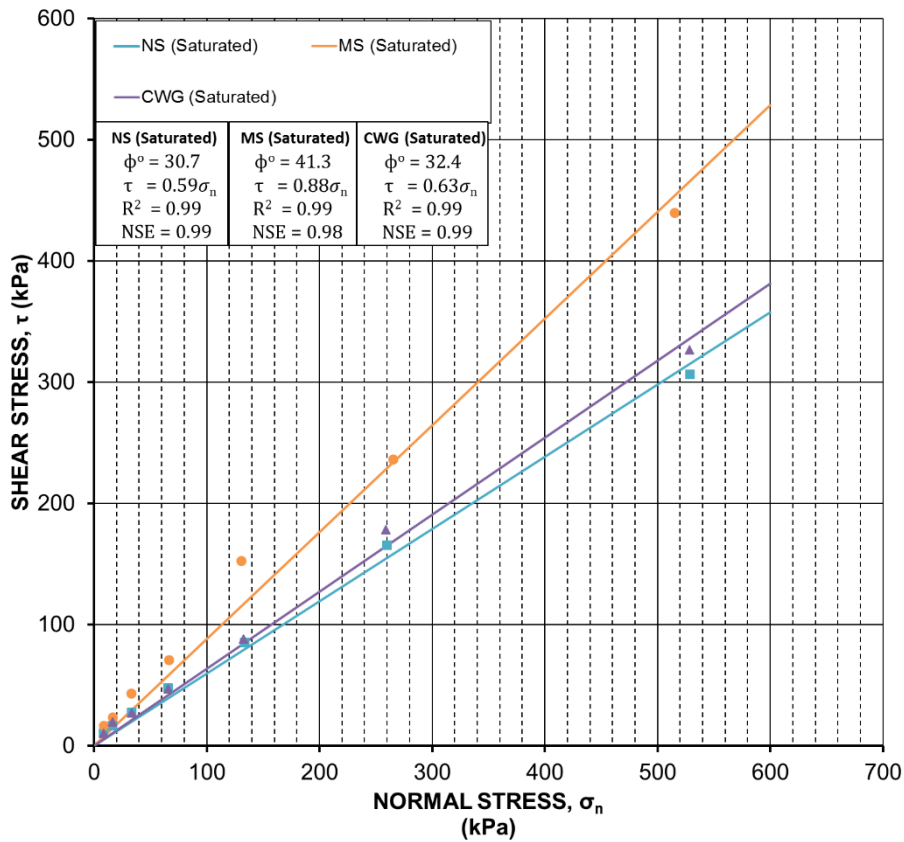
307

**Fig.5.** Peak shear strength envelopes of the materials under saturated conditions



308  
309

**Fig. 6.** Final shear strength envelopes of the materials under dry conditions



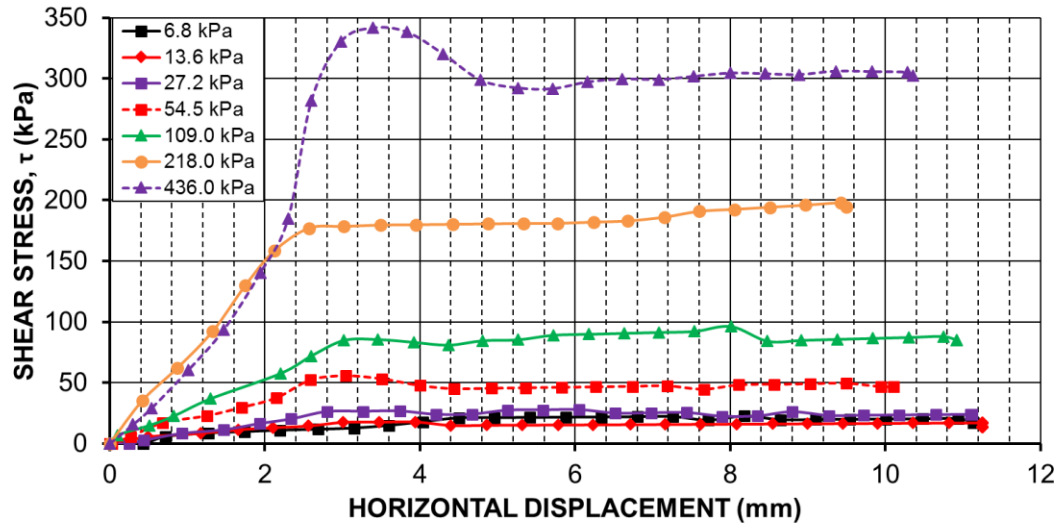
310  
311  
312

**Fig. 7.** Final shear strength envelopes of the materials under saturated conditions

313 The results of the direct shear tests under saturated conditions demonstrated a marginal decline  
314 in the peak friction angle of NS and MS; potentially due to reduced inter-particle friction  
315 caused by the introduction of water molecules between the pores of sands. The reduction of  
316 friction angle under saturated condition was expected and is consistent with previously  
317 published studies (McKelvey et al., 2002). However, interestingly, the peak and final friction  
318 angle of CWG was found to be relatively higher under saturated conditions compared to that  
319 under dry, which is contrary to typical observation in soils. The potential reason for this finding  
320 could be attributed to the adhesion between water and glass particles. When submerged in  
321 water, the surfaces of silicate glass acquire a negative surface charge density through the  
322 dissociation of terminal silanol groups Behrens & Grier (2001), resulting in the development  
323 of adhesion between glass and water particles due to their polarity. Physically, this  
324 phenomenon could potentially be explained by considering the capillary action of water in a  
325 glass tube, leading to the formation of the meniscus. Being polar in nature, glass and water  
326 manifest adhesion at interface greater than the cohesion of individual water molecules; thus,  
327 forming a meniscus.

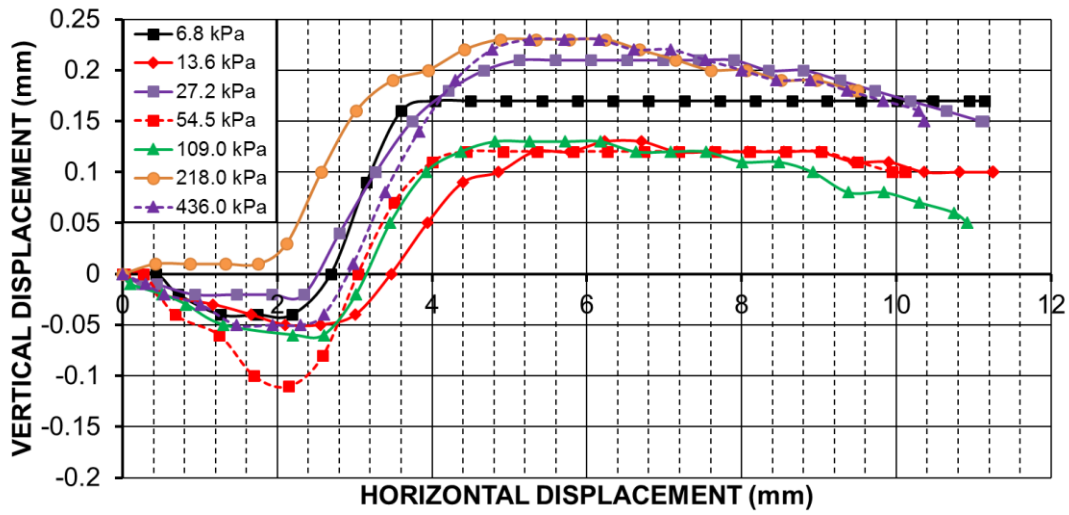
328 Figure 8a and 9a illustrate the shear strength-horizontal displacement behaviour of NS under  
329 dry and saturated conditions, respectively. Figure 8b and 9b represent the horizontal-vertical  
330 displacement behaviour of NS under dry and saturated conditions, respectively. The shear  
331 stress-horizontal displacement behaviour of NS in both dry and saturated conditions showed  
332 that a shear displacement of within 5.0 mm (shear strain of within 0.15) was adequate to  
333 mobilise the peak shear stress under the majority of normal loads. It was also noted that the  
334 shear stress in NS samples non-linearly increased with an increase in horizontal displacement  
335 under both dry and saturated conditions. However, the effect of normal stress on the shear stress  
336 of NS samples was relatively pronounced at higher normal stresses when a distinct peak  
337 appeared. Figure 10a and 11a represent the shear strength-horizontal displacement behaviour  
338 of MS under dry and saturated conditions, respectively. Figure 10b and 11b represent the  
339 horizontal-vertical displacement behaviour of MS under dry and saturated conditions,  
340 respectively. The shear stress-horizontal displacement graph of MS in both dry and saturated  
341 conditions indicated that a relatively higher shear displacement, typically greater than 6 mm,  
342 was required to mobilise peak shear stress under most of the normal stresses. Simultaneously,  
343 it was typically noted that the peak shear stress of NS was similar to its final shear stress. Figure  
344 12a and 13a illustrate the shear strength-horizontal displacement behaviour of CWG under dry  
345 and saturated conditions, respectively. Figure 12b and 13b represent the horizontal-vertical  
346 displacement of CWG under dry and saturated conditions, respectively. In both dry and  
347 saturated conditions, the shear stress-horizontal displacement curve of CWG showed that a  
348 relatively lower shear displacement was required to mobilise the peak shear stress under the  
349 majority of the normal stresses. The peak shear stress mobilised at around 4.0 mm shear  
350 displacement, and the final vertical displacement mostly reached constant values.

351 Furthermore, the potential reasons for the obtained friction angles of the materials were  
352 afterwards studied using the mineralogical and morphological analysis to examine the chemical  
353 composition and particle shape of each material, respectively.



354  
355

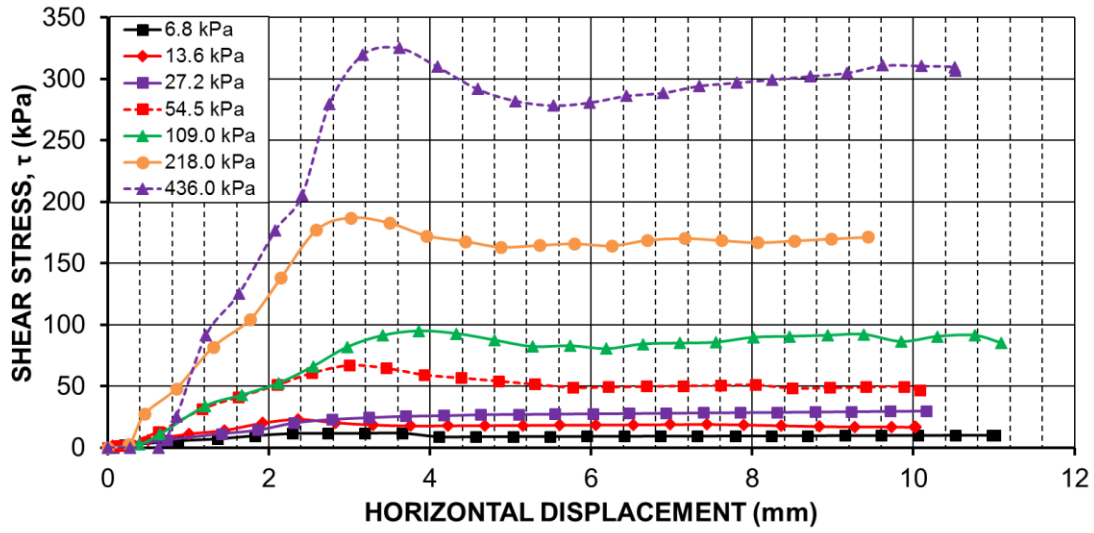
(a)



356  
357

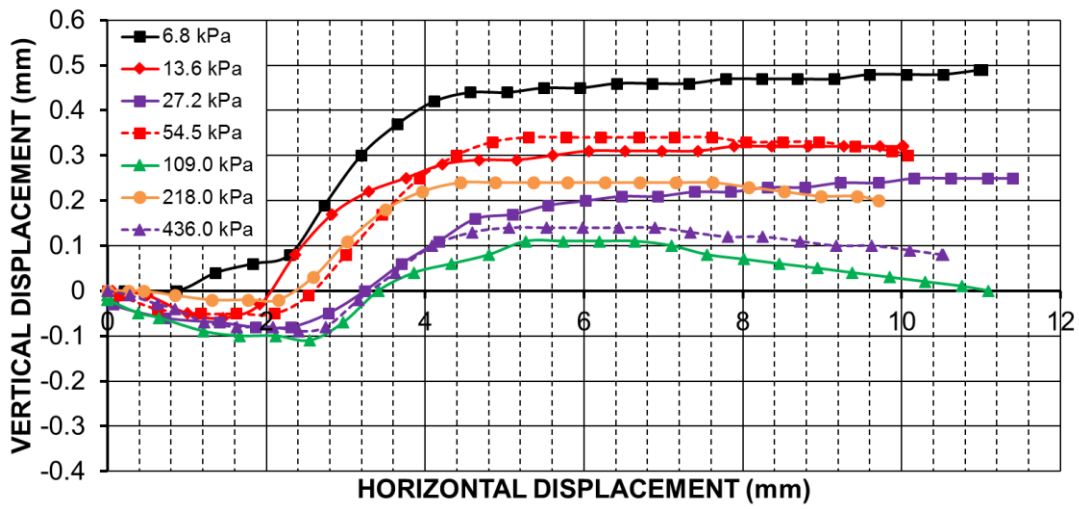
(b)

358 **Fig. 8 (a)** Shear stress-horizontal displacement behaviour of NS under dry conditions  
359 **(b)** Horizontal-vertical displacement behaviour of NS under dry conditions



360  
361

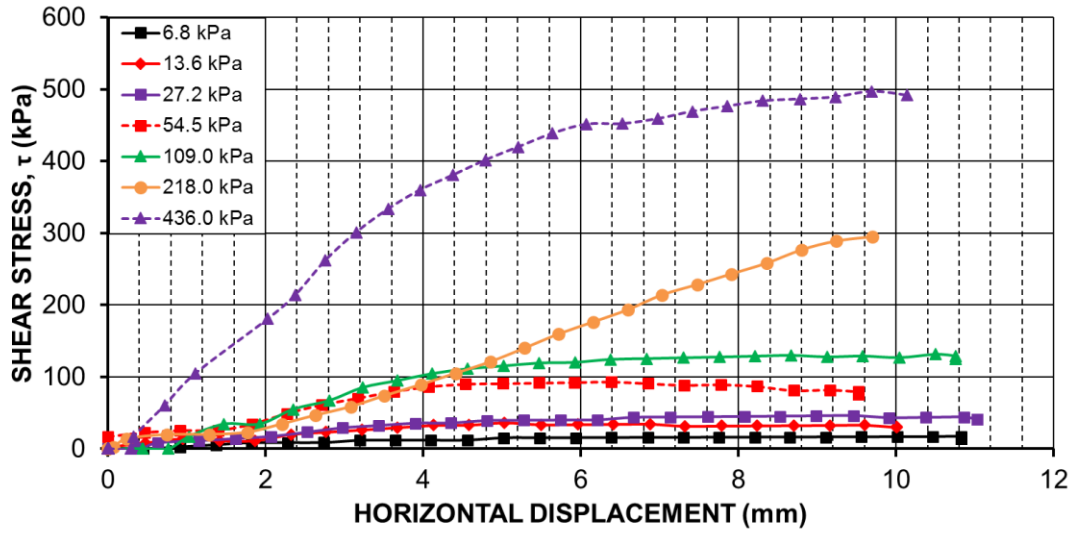
(a)



362  
363

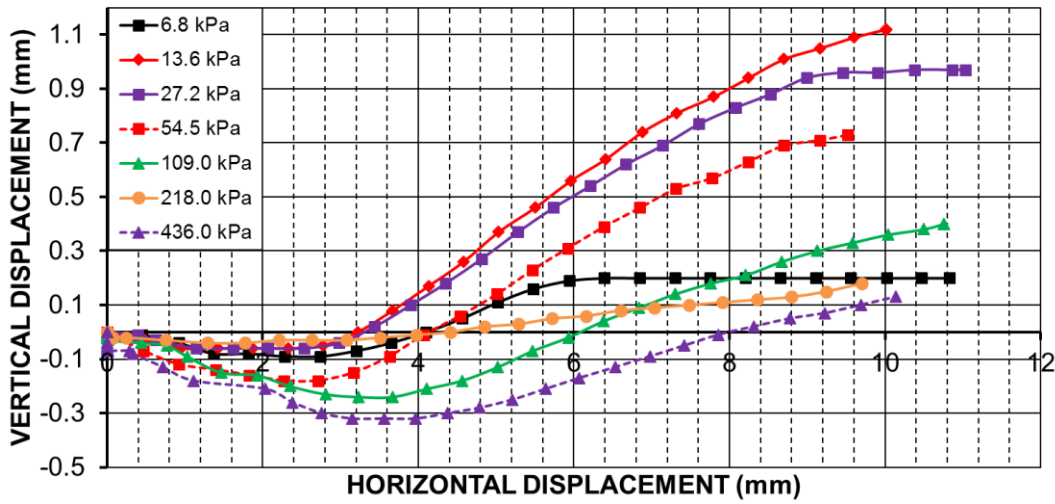
(b)

364 **Fig.9 (a)** Shear stress-horizontal displacement behaviour of NS under saturated conditions  
365 **(b)** Horizontal-vertical displacement behaviour of NS under saturated conditions



366  
367

(a)

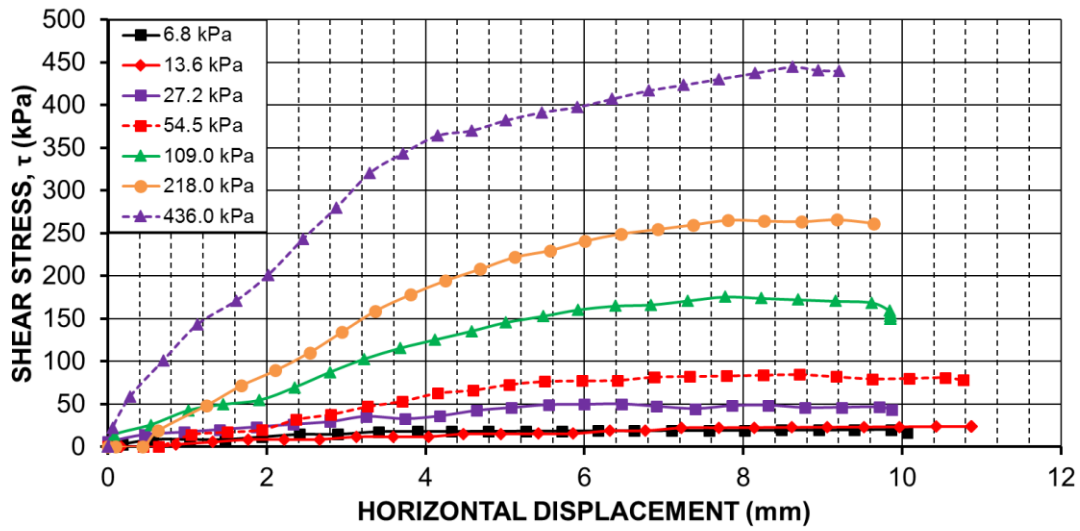


368  
369

(b)

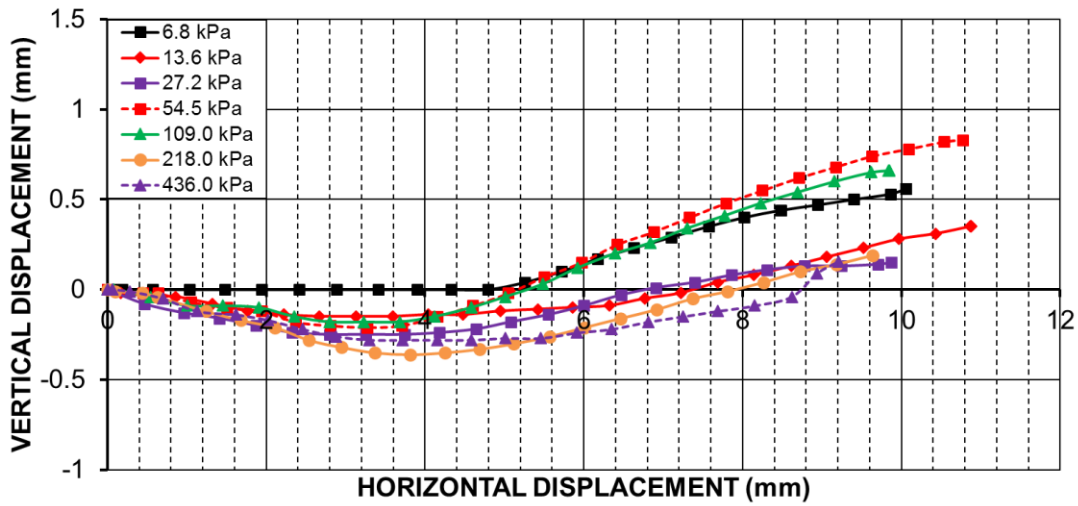
370 **Fig.10 (a)** Shear stress-horizontal displacement behaviour of MS under dry conditions  
371 **(b)** Horizontal-vertical displacement behaviour of MS under dry conditions

372  
373  
374



375  
376

(a)



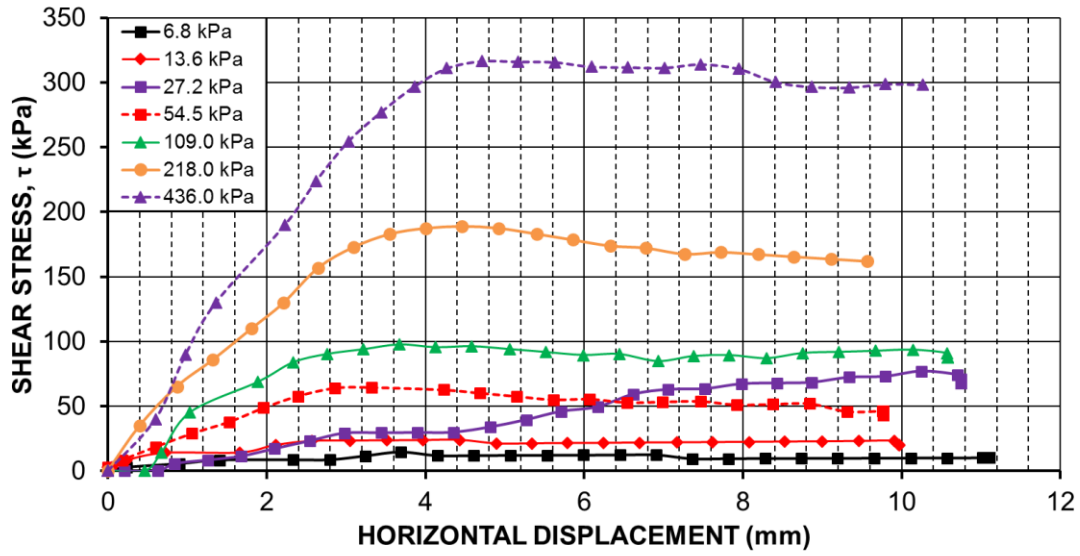
377  
378

(b)

379 **Fig.11 (a)** Shear stress-horizontal displacement behaviour of MS under saturated conditions  
380 **(b)** Horizontal-vertical displacement behaviour of MS under saturated conditions

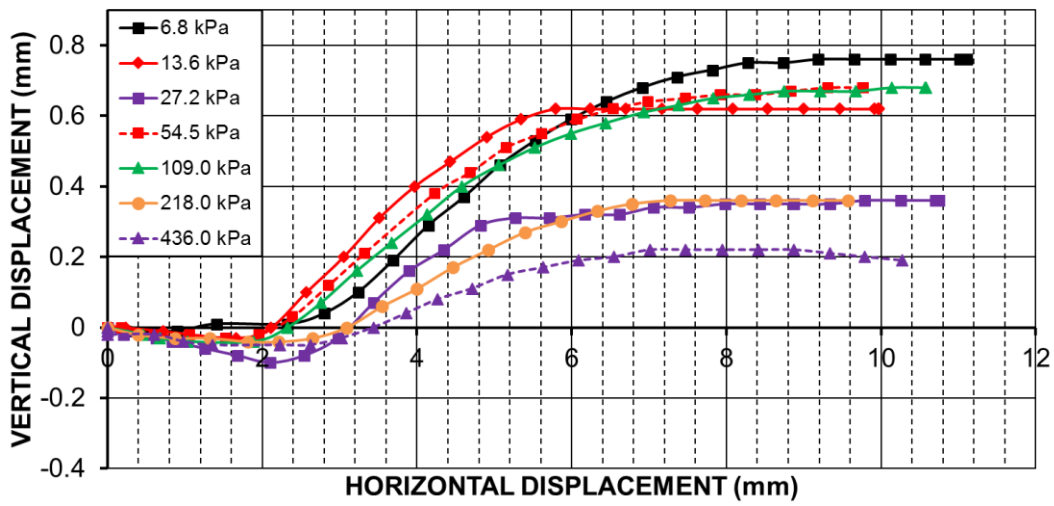
381  
382





383  
384

(a)

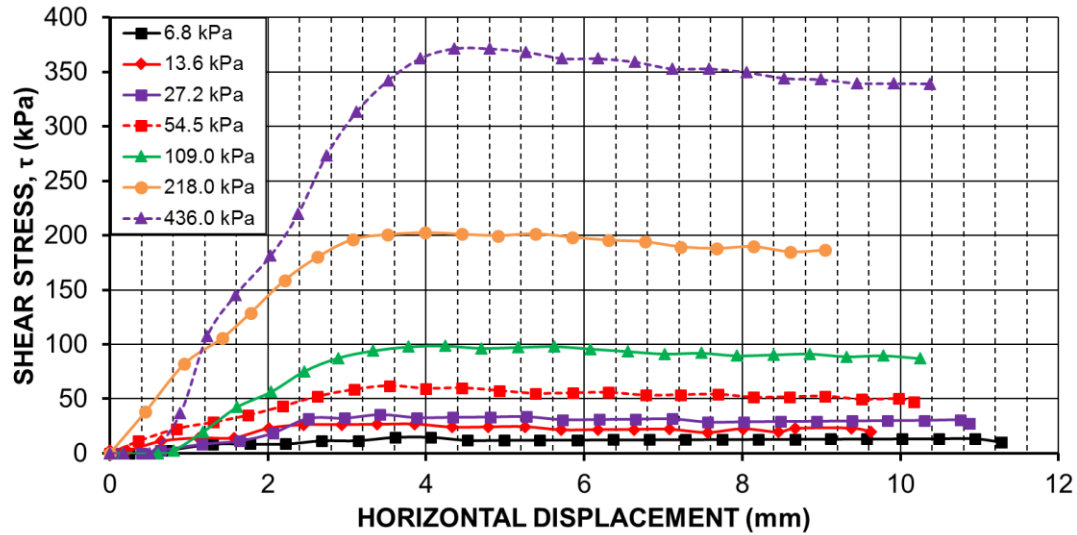


385  
386

(b)

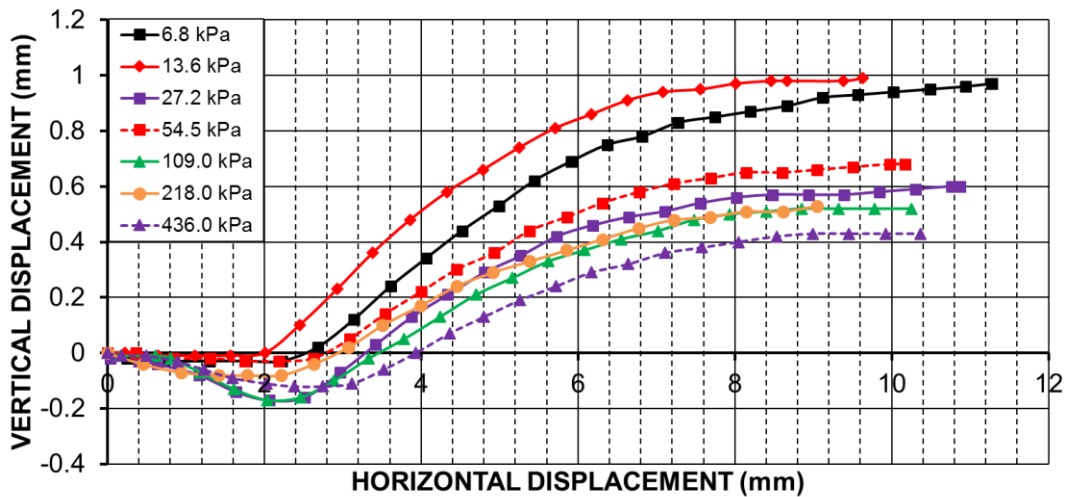
387 **Fig.12 (a)** Shear stress-horizontal displacement behaviour of CWG under dry conditions  
388 **(b)** Horizontal-vertical displacement behaviour of CWG under dry conditions

389  
390



391  
392

(a)



393  
394

(b)

395 **Fig.13 (a)** Shear stress-horizonal displacement behaviour of CWG under saturated conditions  
396 **(b)** Horizontal-vertical displacement behaviour of CWG under saturated conditions

397 **4.2 X-ray fluorescence spectroscopy for the mineralogical analysis**

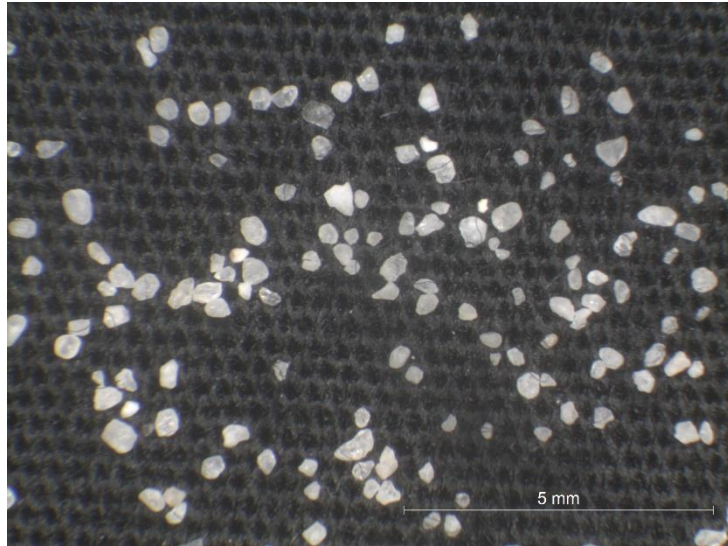
398 The mineralogical analysis of the materials was conducted to determine their elemental  
399 composition, particularly the silica (SiO<sub>2</sub>) content. Silica is the second-most abundant mineral  
400 found on Earth (Patel & Vashi, 2015). Typically, silica comes in the form of quartz and serves  
401 as the most common mineral component of sand, offering higher crushing resistance (Altuhafi  
402 et al., 2016). Silica is a hard and chemically inert mineral exhibiting a high melting point  
403 (Durowaye et al., 2017). Besides performing the mineralogical characterisation, a key  
404 motivation to perform the elemental analysis was to explore the similarity in the chemical  
405 composition of NS, MS and CWG. The results of XRF spectroscopy demonstrated that silica  
406 is the primary mineral in all three materials, with the highest concentration present in NS  
407 (99.81%) followed by CWG (72.07%) and MS (67.74%). These XRF spectroscopy results  
408 show that CWG has a chemical composition comparable to traditional sands (see Table 4).

**Table 4.** Mineralogical analysis of materials performed using XRF spectroscopy.

Oxide concentration	Units	NS	MS	CWG
SiO <sub>2</sub>	%	99.81	67.74	72.07
TiO <sub>2</sub>	%	0.06	0.67	0.05
Al <sub>2</sub> O <sub>3</sub>	%	<0.01	16.17	1.45
Fe <sub>2</sub> O <sub>3</sub>	%	0.05	5.81	0.34
MnO	%	<0.01	0.12	0.01
MgO	%	0.03	2.13	0.69
CaO	%	0.01	1.38	11.09
Na <sub>2</sub> O	%	<0.01	1.71	13.73
K <sub>2</sub> O	%	0.01	3.72	0.33
P <sub>2</sub> O <sub>5</sub>	%	0.01	0.16	0.03
SO <sub>3</sub>	%	0.01	0.24	0.09
V <sub>2</sub> O <sub>5</sub>	ppm	9	177	20
Cr <sub>2</sub> O <sub>3</sub>	ppm	11	97	539
ZnO	ppm	5	122	72
SrO	ppm	2	133	155
BaO	ppm	26	920	355
Co <sub>3</sub> O <sub>4</sub>	ppm	42	18	26
NiO	ppm	8	42	4
CuO	ppm	<2	37	4

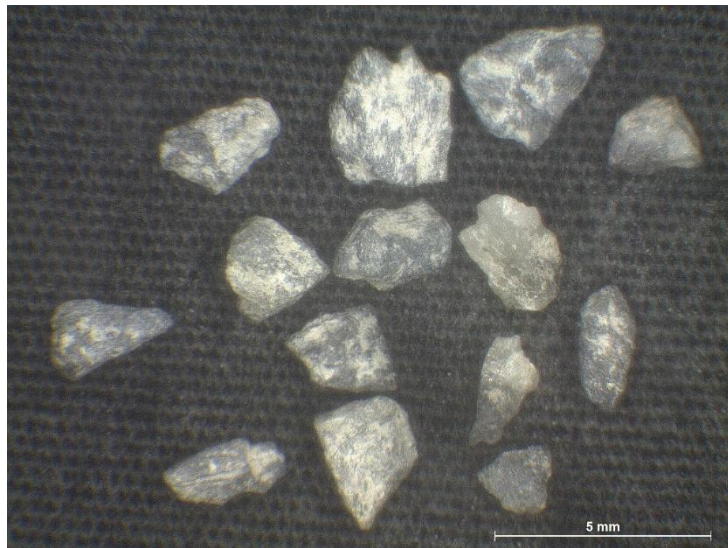
#### 4.3 Microscopic analysis for particle shape quantification

Figure 14, 15 and 16 show the optical microscopy (OM) images containing particles of NS, MS and CWG, respectively. The statistical results obtained using CLT showed that, as the sample size became larger, the distribution of sample means for all three materials approached a normal distribution, which is consistent with the theory of CLT. The skewness and kurtosis of data were calculated to choose the most representative value of particles' roundness index. As the skewness for a perfectly normal distribution is 0, it was seen that the skewness of sample means distribution for all three materials progressively decreased with an increasing number of particles per sample. The acceptable range of skewness for normal distribution lies between -1 to +1 (Chan, 2003). For all given materials, it was noted that the skewness of sample mean distribution was relatively closer to 0 in samples with 25 particles each; potentially indicating a normal distribution. The chi-square goodness of fit test was used to test whether the data with 25 particles come from a normal distribution. The p-value was found to be much larger than the conventional significance level of 0.05, so the null hypothesis was retained that the data is normally distributed. Thus, the mean roundness index corresponding to a sample size of 25 particles per sample was selected for all three materials. Figure 17, 18 and 19 represents the frequency distribution of sample means for roundness index of NS, MS and CWG, respectively. Table 5 represents the statistical results obtained using CLT.



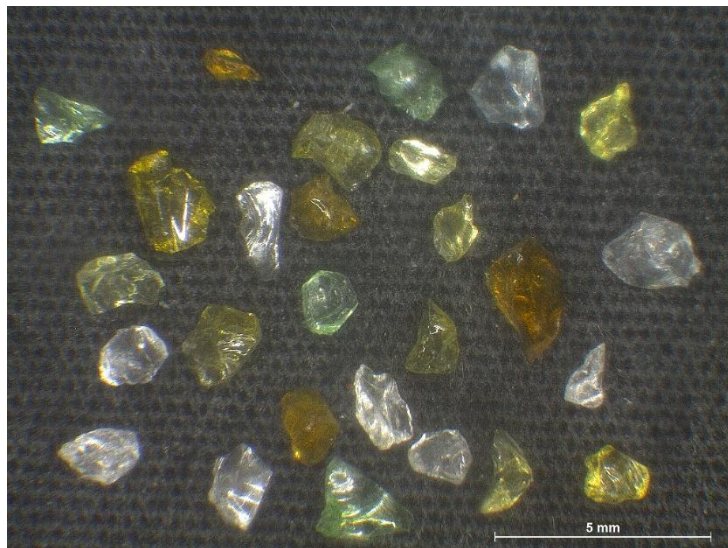
428  
429

**Fig.14.** Micrograph of NS particles



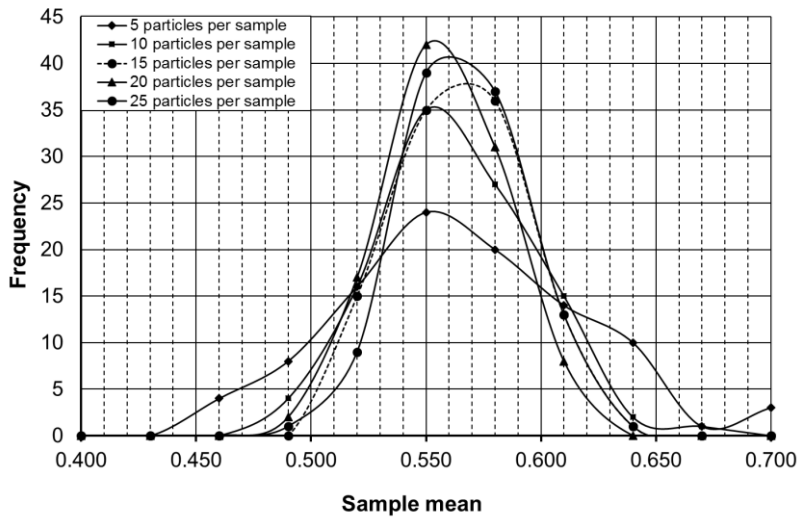
430  
431

**Fig.15.** Micrograph of MS particles



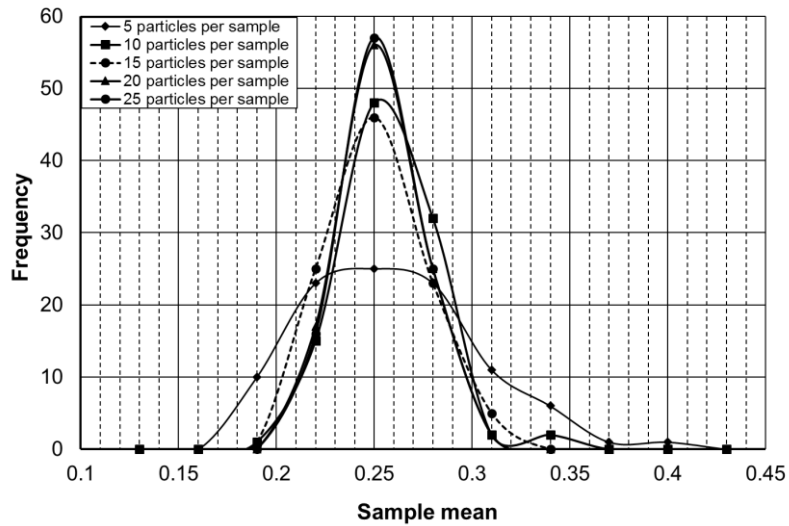
432  
433

**Fig.16.** Micrograph of CWG particles



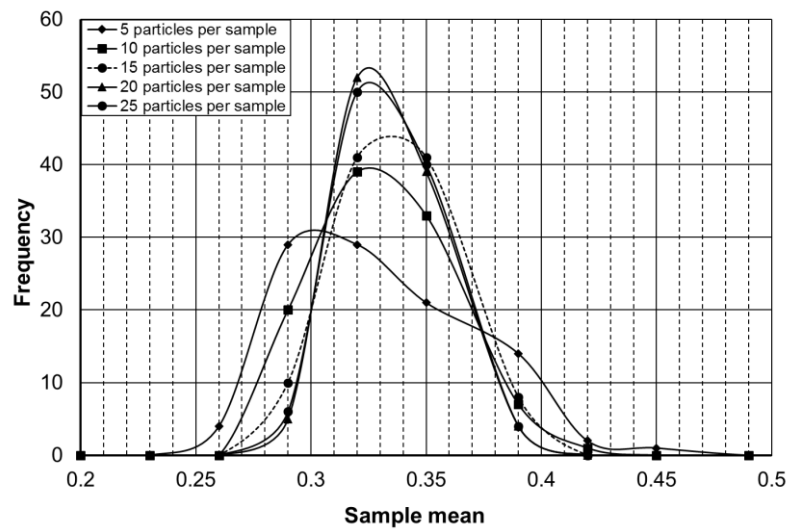
434  
435

**Fig. 17.** Frequency distribution curve for the roundness index of NS



436  
437

**Fig. 18.** Frequency distribution curve for the roundness index of MS



438  
439

**Fig. 19.** Frequency distribution curve for the roundness index of CWG

440 **Table 5.** Statistical results obtained using CLT

No of particles per sample	NS		MS		CWG	
	Skewness	Kurtosis	Skewness	Kurtosis	Skewness	Kurtosis
5	0.342	-0.187	0.638	0.354	0.678	0.571
10	0.262	0.031	0.479	0.803	0.470	0.844
15	0.110	-0.500	0.396	-0.162	0.236	-0.083
20	0.045	-0.356	0.249	0.151	0.058	-0.137
25	-0.006	0.116	0.086	-0.254	0.036	-0.378

441 The results of the morphological analysis showed that MS has the highest particle angularity,  
 442 with a roundness index of 0.24, followed by CWG and NS. Table 6 represents the roundness  
 443 index of the three materials.

444 **Table 6.** Roundness indices of materials calculated using morphological analysis

Material	NS	MS	CWG
Roundness index	0.55	0.24	0.32

445 **Discussion**

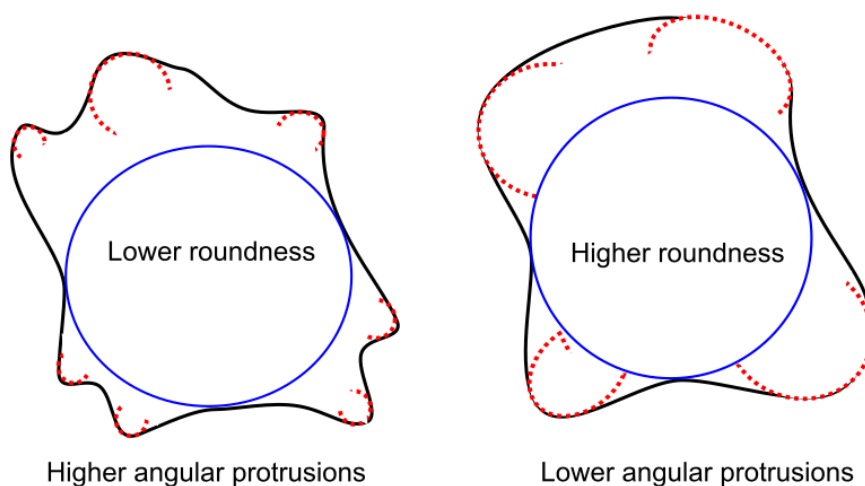
446 The geotechnical characterisation tests demonstrated that CWG exhibits a behaviour similar to  
 447 NS and MS at given particle size and gradation. It was observed that the specific gravity of  
 448 CWG was close to that of the other two sands. The potential reason for this finding could be a  
 449 similarity in the chemical composition of all three materials, noting that silica is the dominant  
 450 mineral in all three materials, as evidenced by the mineralogical analysis. Glass is typically a  
 451 derivative of natural sand, meaning CWG is expected to show a chemical composition  
 452 comparable to traditional sands. Likewise, the densities of all three materials were found to be  
 453 comparable to each other. The potential reason for a relatively higher maximum dry density of  
 454 MS could be the well-graded gradation and higher particle angularity, as demonstrated by the  
 455 gradation and morphological analysis, respectively. Since NS is a uniformly graded material,  
 456 exhibiting relatively higher particle roundness, its maximum dry density turned out to be the  
 457 lowest of all three materials studied. Importantly, it was observed that CWG outperformed the  
 458 other two sands in hydraulic conductivity and abrasion testing. It was noted that the hydraulic  
 459 conductivity of CWG was highest among all three materials; indicating a potential to offer  
 460 favourable drainage behaviour in various geotechnical applications. This point is also endorsed  
 461 by the findings of previous studies, favouring the use of CWG as a drainage media in various  
 462 applications, such as retaining walls, footing drains, French drains and drainage blanket  
 463 (Wartman et al., 2004). The potential reason for a higher permeability of CWG is the non-  
 464 porous and smooth surfaces of its particles which do not hold moisture alongside a lack of clay-  
 465 sized particles in the recycled glass mixtures (Clean Washington Center, 1998).

466 The abrasion testing showed that the abrasion resistance of CWG was nearly two and four  
 467 times superior to NS and MS, respectively. The relatively superior abrasion resistance of CWG  
 468 could be particularly beneficial to applications where the materials are subjected to impact,  
 469 potentially increasing the structural durability due to reduced wear and tear. Besides technical  
 470 benefits, the higher abrasion resistance of CWG could be helpful during the logistics, such as  
 471 transportation, handling and installation.

472 The shear strength testing of materials showed that the friction angle of CWG is comparable to  
 473 traditional sands. It was found that MS has the highest peak friction angle under saturated  
 474 conditions, followed by CWG and NS. Typically, the friction angle of sands is relatively lower  
 475 under saturated conditions than under dry conditions, due a to greater inter-particle lubrication.

476 However, surprisingly, it was observed that the friction angle of CWG was considerably higher  
477 under saturated conditions than under dry conditions, showing an increase of nearly 10%,  
478 potentially due to a greater adhesion between water and CWG particles. This increase in the  
479 saturated friction angle of CWG could be favourable for applications where the moisture  
480 content is high and keep fluctuating. Since the peak and final friction angle of MS was found  
481 to be the highest of all three materials, the potential reasons for this finding could be the well-  
482 graded gradation, relatively large mean particle size and higher particle angularity of MS.

483 Morphologically, digital image analysis was performed to analyse the particle shape of the  
484 materials using an optical microscope. Particle shape is an essential parameter in the fields of  
485 civil engineering and geology due to its significant impact on the physical behaviour of soils  
486 (Lees, 1964). Several researchers have attempted to develop descriptors to quantify the shape  
487 of particles, including the normalised shape factor (SF) proposed by Sukumaran & Ashmawy  
488 (2001), the fractal dimension proposed by Vallejo & Zhou (1995) and the ruggedness factor  
489 proposed by Wettimuny & Penumadu (2004). However, due to a long history and consistent  
490 use, the most accepted method for particle shape quantification was developed by Wadell in  
491 1932 (Zheng & Hryciw, 2016). Wadell (1932) used the term roundness and defined it as the  
492 mean radius of curvature of surface features relative to the radius of the largest sphere that can  
493 be inscribed in the grain. Roundness is typically sensitive to the sharpness of angular  
494 protrusions from the grain; yielding higher values for smooth grains and lower values for the  
495 rough ones (Bowman et al., 2001). Figure 20 exemplifies the roundness of a particle in terms  
496 of angular protrusions. Studies show that the angularity, which denotes variations at the corners  
497 of particles, plays a pivotal role in promoting interlocking between particles (Hossain et al.,  
498 2007; Zhao et al., 2015). Holubec & D'appolonia (1973) tested the effect of particle shape on  
499 the geotechnical engineering parameters of granular soils and concluded that granular materials  
500 with the same relative density could manifest significantly different behaviour due to variation  
501 in particle angularity. Some studies show that particle breakage is often guided by particle  
502 angularity (shape) rather than size (Lackenby, 2006). Qing-bing et al. (2011) studied the effect  
503 of particle shape on the shear strength behaviour of three different sands. Their study found  
504 that the critical friction angle of sand reduces linearly with an increase in particle roundness.  
505 Similarly, Shinohara et al. (2000) showed a direct relationship between particle angularity and  
506 friction angle, suggesting that angular particles offer greater interlock than rounded ones.



508 **Fig. 20.** Effect of angular protrusions on the roundness of the particle (adapted from  
509 Hawkins, 1993)

510 The results of the morphological analysis showed that MS has the highest particle angularity,  
511 followed by CWG and NS. Typically, the particle shape of materials is not analysed

512 quantitatively for geotechnical applications. However, the results of a few studies show that  
513 angular sands tend to exhibit a larger friction angle, higher maximum and minimum void ratios,  
514 and greater compressibility potential, compared to their rounded counterparts under similar  
515 conditions (Muszynski & Vitton, 2012). It was observed that the particle angularity of CWG  
516 was markedly higher than that of NS and relatively closer to that of MS. In other civil  
517 engineering applications, such as concrete, the higher angularity of aggregates is not always  
518 desirable, as it could reduce the workability of fresh concrete. However, the relatively higher  
519 particle angularity of CWG could directly help improve the structural stability in numerous  
520 geotechnical applications; favouring the potential use of CWG as an alternative geomaterial.

521 The calculated roundness indices were classified using particle roundness grades as suggested  
522 by Russell & Taylor (1937), classifying particles into five distinct classes of shape using the  
523 roundness estimates of Wadell (1932). It was found that NS has a rounded particle shape,  
524 whereas MS turned out to be sub-angular. The particle shape of CWG was found to be sub-  
525 rounded. These results are comparable to the findings of some previous studies reporting the  
526 roundness indices of different sands. For example, Cho et al. (2006) calculated the roundness  
527 index of various natural sands. Their study found that the roundness index of Nevada and  
528 sandboil sand was found to be 0.60 and 0.55 respectively, which is similar to the roundness  
529 index of NS, 0.55, obtained in this study.

530 Interestingly, it was noted that the roundness indices of CWG and MS were relatively closer to  
531 each other, with a difference of nearly 28%, indicating a relatively higher particle angularity in  
532 both materials. These results are consistent with the findings of some previous studies,  
533 suggesting that natural sands tend to have rounded shape, whereas manufactured sands have  
534 angular particles (Kumar, 2016). Since the natural sand was sourced from a beach, it was  
535 expected to contain rounded grains, as roundness is predominantly caused by abrasion during  
536 sediment transport (Nichols, 2009). Likewise, some previous studies confirmed that  
537 manufactured sands have relatively higher particle angularity Chetia et al. (2017); potentially  
538 due to relatively lower exposure to abrasion compared to natural sands, which are subjected to  
539 erosion due to wave and aeolian action. Since CWG is obtained by crushing and processing of  
540 waste glass, the particle shape of CWG is expected to be relatively angular (So et al., 2016).  
541 This study found that the particle shape of CWG is sub-rounded, lying midway between that  
542 of NS and MS. Considering the brittle nature of CWG, a potential reason for its sub-rounded  
543 classification could be the particle breakage due to attrition, causing a change in shape from  
544 angular to sub-rounded particles (Dhir et al., 2018).

545 Despite the findings described above, it is vital to consider the effect of particle size on the  
546 geotechnical performance of granular materials. Several previous studies have shown that well-  
547 graded sands with large particles tend to exhibit relatively greater shear strength. Bareither et  
548 al. (2008) investigated the effects of physical characteristics on the shear strength of different  
549 compacted sands. Their study observed that well-graded sands with large particles showed the  
550 highest friction angles. Islam et al. (2019) examined the impact of particle size on the shear  
551 strength behaviour of sands using a direct shear machine. Their study found that the friction  
552 angle increased with increase in particle size for well-graded sands. Similarly, Dai et al. (2016)  
553 analysed the effect of particle size on the friction angle of different uniformly-graded glass  
554 beads. Their study reported that the peak friction angle of glass beads increased and showed a  
555 more dilative shearing response with increasing mean particle size ( $D_{50}$ ), concluding that  
556 particle size may influence the shear strength behaviour of granular materials. However, these  
557 findings for granular materials may not necessarily correspond to CWG. Disfani et al. (2011b)  
558 analysed the geotechnical behaviour of three types of CWG, categorised based on their  
559 maximum particle size, which was 4.75, 9.5 and 19 mm. Their study observed that the  
560 geotechnical behaviour of CWG deteriorates at coarser particle size because of several reasons,



561 including its low ability to hold and absorb water, substantial changes in gradation curves pre  
562 and post-compaction, and relatively higher segregation potential. It was concluded that CWG  
563 with coarse particles reduces its potential for use in geotechnical engineering applications.  
564 However, the same study reported that CWG with fine and medium-sized particles offered  
565 superior geotechnical behaviour, comparable to traditional sand, and could potentially be used  
566 in a range of geotechnical applications.

567 Currently, the use of CWG in traditional geotechnical applications is relatively under-  
568 researched (Kazmi et al., 2019b). Secondly, there are presently limited suppliers of CWG in  
569 Australia offering CWG for recycling applications. Once the geotechnical applications of  
570 CWG are fully developed, its acceptance and availability would be expected to increase, and  
571 its price would be expected to drop due to increased market competition. Presently, the major  
572 barrier to the use of CWG in geotechnical engineering projects is a lack of knowledge on its  
573 geotechnical behaviour Disfani et al. (2011b); potentially indicating a research gap. Greater  
574 use of CWG would help the recycling companies dispose of thousands of tonnes of waste glass  
575 that is currently being sent to landfills or stockpiled. Lastly, due to the environment-friendly  
576 nature and growing focus on sustainability, the secondary use of CWG is expected to gain  
577 greater acceptance.

578 Despite huge potential, no formal study has been found exploring the use of CWG as backfill  
579 in stone column construction (Zukri & Nazir, 2018). Therefore, in continuation to this research  
580 and for the first time, a separate study will be presented in future to examine the geotechnical  
581 behaviour of CWG as a next-generation alternative to traditional sands for use as a column  
582 backfill in granular pile construction. Technically, the next stage of this research will involve  
583 investigating the geotechnical performance of “glass column”, made with CWG and installed  
584 in weak soil, as opposed to the traditional sand/stone columns used for ground improvement.  
585 Presumably, the challenges typically associated with the use of CWG in concrete, such as  
586 alkali-silica reaction and workability issues, will not dominate if CWG is used to backfill  
587 ground columns; potentially replacing traditional sand in a typical geotechnical application.

## 588 **Conclusion**

589 This study compared the geotechnical, mineralogical and morphological behaviour of CWG  
590 with that of NS and MS. Overall, it was observed that the behaviour of CWG is similar, or  
591 sometimes even superior, to traditional construction sands at given particle size and gradation.  
592 The geotechnical characterisation tests showed that CWG has similar behaviour to NS and MS,  
593 with CWG exhibiting superior permeability and abrasion resistance. Potential reasons for a  
594 comparable geotechnical behaviour of CWG and traditional sands could be their similar  
595 chemical composition and specific gravity, alongside the relatively angular particle shape of  
596 CWG. Moreover, as opposed to the typical observation, the shear strength testing showed that  
597 the friction angle of CWG increased under saturated conditions compared to that under dry;  
598 potentially showing its stability under saturated conditions. However, the geotechnical  
599 behaviour of CWG could be sensitive to its particle size and possibly deteriorate when its  
600 particle size becomes coarser, suggesting the need to determine the critical particle size of  
601 CWG beyond which its geotechnical performance may start to drop. Therefore, building on the  
602 findings of this paper and for the first time, a separate study will be presented in future that will  
603 systematically investigate and compare the geotechnical performance of CWG, as a sustainable  
604 alternative to NS and MS, for use as a column backfill in granular pile construction.  
605 Importantly, the use of CWG as an alternative geomaterial will potentially support the cleaner  
606 production concept by encouraging the use of waste glass and reducing carbon emissions. For  
607 future research, this study suggests performing a detailed techno-economic and life-cycle  
608 analysis of CWG for use in geotechnical engineering applications.

609 **Acknowledgments**

610 The authors would like to thank Peter Lovegrove (Enviro Sand, Australia) for supplying the  
611 crushed waste glass used in this study. The authors are also grateful to Anthony Neary  
612 (Department of Transport and Main Roads, Queensland, Australia) for his assistance with the  
613 abrasion testing of the materials. Special thanks go to Mark Raven (X-ray Fluorescence  
614 Laboratory at CSIRO, Australia) for his help with the mineralogical study of the test materials.  
615 Gratitude also goes to Jonathan Read (School of Mechanical and Mining Engineering at The  
616 University of Queensland, Australia) for his support with the microscopic imaging of the  
617 materials. Lastly, special thanks go to Sebastian Quintero (Geotechnical Engineering  
618 Laboratory at The University of Queensland, Australia) for his assistance with the geotechnical  
619 testing of the materials.

620 **Funding**

621 This research did not receive any specific grant from funding agencies in the public,  
622 commercial, or not-for-profit sectors.

623  
624  
625  
626  
627  
628  
629  
630  
631  
632  
633  
634  
635  
636  
637  
638  
639  
640  
641  
642  
643  
644  
645  
646  
647  
648  
649  
650  
651  
652  
653  
654

**References**

- 656 1. Altuhafi, C., Georgiannou, V., 2016. Effect of particle shape on the mechanical  
657 behavior of natural sands. *Journal of Geotechnical and Geoenvironmental Engineering*.  
658 142 (12), 040160711-15.
- 659 2. Amiri, S., Nazir, R., Dehghanbanadaki, A., 2018. Experimental study of geotechnical  
660 characteristics of crushed glass mixed with kaolinite soil. *International Journal of*  
661 *Geomate*. 14 (45), 170-176.
- 662 3. Arulrajah, A., Ali, M., Disfani, M., Piratheepan, J., Bo, M., 2012a. Geotechnical  
663 performance of recycled glass-waste rock blends in footpath bases. *Journal of Materials*  
664 *in Civil Engineering*. 25 (5), 653-661.
- 665 4. Arulrajah, A., Disfani, M., Maghoolpilehrood, F., Horpibulsuk, S., Udonchai, A.,  
666 Imteaz, M., Du, Y., 2015. Engineering and environmental properties of foamed  
667 recycled glass as a lightweight engineering material. *Journal of Cleaner Production*. 94,  
668 369-375.
- 669 5. Arulrajah, A., Piratheepan, J., Disfani, M., Bo, M., 2012b. Geotechnical and  
670 geoenvironmental properties of recycled construction and demolition materials in  
671 pavement subbase applications. *Journal of Materials in Civil Engineering*. 25 (8), 1077-  
672 1088.
- 673 6. Bareither, C., Edil, T., Benson, C., Mickelson, D., 2008. Geological and physical  
674 factors affecting the friction angle of compacted sands. *Journal of Geotechnical and*  
675 *Geoenvironmental Engineering*. 134 (10), 1476-1489.
- 676 7. Behrens, S., Grier, D., 2001. The charge of glass and silica surfaces. *The Journal of*  
677 *Chemical Physics*. 115 (14), 6716-6721.
- 678 8. Bogas, J., de Brito, J., Figueiredo, J., 2015. Mechanical characterization of concrete  
679 produced with recycled lightweight expanded clay aggregate concrete. *Journal of*  
680 *Cleaner Production*. 89, 187-195.
- 681 9. Bowman, E., Soga, K., Drummond, W., 2001. Particle shape characterisation using  
682 Fourier descriptor analysis. *Geotechnique*, 51 (6), 545-554.
- 683 10. Bravo, M., De Brito, J., Pontes, J., Evangelista, L., 2015. Mechanical performance of  
684 concrete made with aggregates from construction and demolition waste recycling  
685 plants. *Journal of Cleaner Production*. 99, 59-74.
- 686 11. Carter, R., Yan, Y., 2005. Measurement of particle shape using digital imaging  
687 techniques. *Journal of Physics: Conference Series*. 15, 177-182.
- 688 12. Cement Concrete and Aggregates Australia. (2011). *Performance Benchmarking of*  
689 *Australian Business Regulation: Planning, Zoning and Development Assessments*  
690 Retrieved from [https://www.pc.gov.au/inquiries/completed/regulation-benchmarking-](https://www.pc.gov.au/inquiries/completed/regulation-benchmarking-planning/submissions/sub054.pdf)  
691 [planning/submissions/sub054.pdf](https://www.pc.gov.au/inquiries/completed/regulation-benchmarking-planning/submissions/sub054.pdf) (accessed 18 Aug 2020)
- 692 13. Chan, Y., 2003. Biostatistics 101: Data Presentation. *Singapore medical journal*. 44 (6),  
693 280-285.
- 694 14. Chen, B., Zhu, H., Li, B., Sham, M., Li, Z., 2020. Study on the fire resistance  
695 performance of cementitious composites containing recycled glass cullets (RGCs).  
696 *Construction and Building Materials*. 242, 1179921-9.
- 697 15. Chetia, M., Baruah, M., Sridharan, A., 2017. Effect of quarry dust on compaction  
698 characteristics of clay. *Contemporary Issues in Geoenvironmental Engineering*. 78-  
699 100.
- 700 16. Cho, G., Dodds, J., Santamarina, J., 2006. Particle shape effects on packing density,  
701 stiffness, and strength: natural and crushed sands. *Journal of Geotechnical and*  
702 *Geoenvironmental Engineering*. 132 (5), 591-602.

- 703 17. Clean Washington Center. 1998. A tool kit for the use of post-consumer glass as a  
704 construction aggregate. Report#: GL-97-5. Seattle, WA, USA.
- 705 18. Criss, R., Winston, W., 2008. Do Nash values have value? Discussion and alternate  
706 proposals. *Hydrological Processes*. 22 (14), 2723-2725.
- 707 19. Das, B., 2009. *Principles of Geotechnical Engineering*. Seventh edition, Cengage  
708 Learning.
- 709 20. Dai, B., Yang, J., Zhou, C., 2016. Observed effects of interparticle friction and particle  
710 size on shear behavior of granular materials. *International Journal of Geomechanics*. 16  
711 (1), 040150111-11.
- 712 21. Department of Agriculture, Water and the Environment. 2013. National Waste Report.  
713 Retrieved from:  
714 [https://www.environment.gov.au/protection/waste-resource-recovery/national-waste-](https://www.environment.gov.au/protection/waste-resource-recovery/national-waste-reports/national-waste-report-2013/infrastructure)  
715 [reports/national-waste-report-2013/infrastructure](https://www.environment.gov.au/protection/waste-resource-recovery/national-waste-reports/national-waste-report-2013/infrastructure) (accessed 15 Aug 2020)
- 716 22. Dhir, R., de Brito, J., Ghataora, G., Lye, C., 2018. *Sustainable Construction Materials:*  
717 *Glass Cullet*. Woodhead Publishing.
- 718 23. Dhir, R., de Brito, J., Silva, R., Lye, C., 2019. *Sustainable Construction Materials:*  
719 *Recycled Aggregates*. Woodhead Publishing.
- 720 24. Disfani, M., Arulrajah, A., Ali, M., Bo, M., 2011a. Fine recycled glass: a sustainable  
721 alternative to natural aggregates. *International Journal of Geotechnical Engineering*. 5  
722 (3), 255-266.
- 723 25. Disfani, M., Arulrajah, A., Bo, M., Hankour, R., 2011b. Recycled crushed glass in road  
724 work applications. *Waste Management*. 31 (11), 2341-2351.
- 725 26. Durowaye, S., Sekunowo, O., Lawal, A., Ojo, O., 2017. Development and  
726 characterisation of iron millscale particle reinforced ceramic matrix composite. *Journal*  
727 *of Taibah University for Science*. 11 (4), 634-644.
- 728 27. Dyer, P., Klinsky, L., Silva, S., Lima, M., 2020. Mechanical and structural assessment  
729 of hot mix bituminous mixtures containing waste foundry sand. *International Journal*  
730 *of Pavement Engineering*, 1-12. DOI: <https://doi.org/10.1080/10298436.2020.1724290>
- 731 28. Emery, J. 1974. *Use of Mining and Metallurgical Wastes in Construction*.  
732 Transportation Research Board.
- 733 29. Eurostat .2020. Packaging waste statistics. Retrieved from:  
734 [https://ec.europa.eu/eurostat/statistics-](https://ec.europa.eu/eurostat/statistics-explained/index.php/Packaging_waste_statistics#Waste_generation_by_packaging_material)  
735 [explained/index.php/Packaging\\_waste\\_statistics#Waste\\_generation\\_by\\_packaging\\_m](https://ec.europa.eu/eurostat/statistics-explained/index.php/Packaging_waste_statistics#Waste_generation_by_packaging_material)  
736 [aterial](https://ec.europa.eu/eurostat/statistics-explained/index.php/Packaging_waste_statistics#Waste_generation_by_packaging_material)
- 737 30. Frosch, R., Gallopoulos, N., 1989. Strategies for manufacturing. *Scientific American*.  
738 261 (3), 144-153.
- 739 31. Ganti, A., 2019. Central Limit Theorem (CLT). Retrieved from:  
740 [https://www.investopedia.com/terms/c/central\\_limit\\_theorem.asp](https://www.investopedia.com/terms/c/central_limit_theorem.asp)
- 741 32. Hazen, A., 1892. Some physical properties of sands and gravels, with special reference  
742 to their use in filtration. 24th Annual Rep., Publ. Doc. no. 34, 539–556, Massachusetts  
743 State Board of Health, Boston, USA.
- 744 33. Hawkins, A., 1993. *The Shape of Powder-Particle Outlines*. Wiley, New York.
- 745 34. Hebhoub, H., Aoun, H., Belachia, M., Houari, H., Ghorbel E., 2011. Use of waste  
746 marble aggregates in concrete. *Construction and Building Materials* 25 (3), 1167-1171.
- 747 35. Holmstrom, O., Swan, C., 1999. Geotechnical properties of innovative, synthetic  
748 lightweight aggregates. 1999 International Ash Utilization Symposium. Center for  
749 Applied Energy Research, University of Kentucky, Paper# 49.
- 750 36. Holubec, I., D'appolonia, E., 1973. Effect of particle shape on the engineering  
751 properties of granular soils. Evaluation of relative density and its role in geotechnical

- 752 projects involving cohesionless soils, ASTM STP 523, American Society for Testing  
753 and Materials. 304-318.
- 754 37. Islam, M., Siddika, A., Hossain, M., Rahman, A., Asad, M., 2019. Effect of particle  
755 size on the shear strength behavior of sands. *Australian Geomechanics*. 46 (3), 75-86.
- 756 38. Jonah, F., Adjei-Boateng, D., Agbo, N., Mensah, E., Edziyie, R., 2015. Assessment of  
757 sand and stone mining along the coastline of Cape Coast, Ghana. *Annals of GIS*. 21  
758 (3), 223-231.
- 759 39. Kaza, S., Yao, L., Bhada-Tata, P., Woerden, F., 2018. *What a Waste 2.0: A Global  
760 Snapshot of Solid Waste Management to 2050*. Urban Development. Washington, DC:  
761 World Bank.
- 762 40. Koehnken, L., Rintoul, M., Goichot, M., Tickner, D., Loftus, A., Acreman, M., 2020.  
763 Impacts of riverine sand mining on freshwater ecosystems: A review of the scientific  
764 evidence and guidance for future research. *River Research and Applications*. 36 (3),  
765 362-370.
- 766 41. Hossain, Z., Indraratna, B., Darve, F., Thakur, P., 2007. DEM analysis of angular  
767 ballast breakage under cyclic loading. *Geomechanics and Geoengineering: An  
768 International Journal*. 2 (3), 175-181.
- 769 42. Jani, Y., Hogland, W., 2014. Waste glass in the production of cement and concrete—A  
770 review. *Journal of Environmental Chemical Engineering*. 2 (3), 1767-1775.
- 771 43. Kazmi, D., Williams, D., Serati, M., 2019a. Comparison of Basic Geotechnical  
772 Parameters of Crushed Waste Glass with Natural and Manufactured Sands. 53<sup>rd</sup> US  
773 Rock Mechanics/Geomechanics Symposium. New York, USA. ARMA-2019-0312.
- 774 44. Kazmi, D., Williams, D., Serati, M., 2019b. Waste Glass in Civil Engineering  
775 Applications – A Review. *International Journal of Applied Ceramic Technology*. 17  
776 (2), 529-554. DOI: <https://doi.org/10.1111/ijac.13434>
- 777 45. Kelly, T., 1998. *Crushed Cement Concrete Substitution for Construction Aggregates -  
778 A Materials Flow Analysis*. US Department of the Interior, US Geological Circular.
- 779 46. Koehnken, L., Rintoul, M., 2018. Impacts of Sand mining on ecosystem structure,  
780 process and biodiversity in rivers. WWF.
- 781 47. Kumar, P., Radhakrishna., 2016. *Characteristics of SCC with Fly Ash and  
782 Manufactured Sand*. *Materials Science and Engineering*. 149 (1), 1-9.
- 783 48. Lackenby, J., 2006. Triaxial behaviour of ballast and the role of confining pressure  
784 under cyclic loading. PhD Thesis, University of Wollongong.  
785 <https://ro.uow.edu.au/theses/516/>
- 786 49. Lee, J., Smith, M., Smith, L., 2007. A new approach to the three-dimensional  
787 quantification of angularity using image analysis of the size and form of coarse  
788 aggregates. *Engineering Geology*. 91 (2-4), 254-264.
- 789 50. Lees, G., 1964. A new method for determining the angularity of particles.  
790 *Sedimentology*. 3 (1), 2-21.
- 791 51. Mahmoud, E., 2005. Development of experimental methods for the evaluation of  
792 aggregate resistance to polishing, abrasion, and breakage. PhD Thesis, Texas A&M  
793 University. <https://oaktrust.library.tamu.edu/handle/1969.1/4959>
- 794 52. Marangoni, M., Secco, M., Parisatto, M., Artioli, G., Bernardo, E., Colombo, P.,  
795 Altiasi, H., Binmajed, M., Binhussain., 2014. Cellular glass—ceramics from a self  
796 foaming mixture of glass and basalt scoria. *Journal of Non-Crystalline Solids*. 403,  
797 38-46.
- 798 53. McKelvey, D., Sivakumar, V., Bell, A., McLaverty, G., 2002. Shear strength of  
799 recycled construction materials intended for use in vibro ground improvement.  
800 *Proceedings of the Institution of Civil Engineers-Ground Improvement*. 6 (2), 59-68.

- 801 54. McCuen, R., Knight, Z., & Cutter, A., 2006. Evaluation of the Nash–Sutcliffe  
802 efficiency index. *Journal of hydrologic engineering*. 11 (6), 597-602.
- 803 55. Mishra, P., Suman, S., Das, S., 2017. Experimental investigation and prediction models  
804 for thermal conductivity of biomodified buffer materials for hazardous waste disposal.  
805 *Journal of Hazardous, Toxic, and Radioactive Waste*. 21 (2), 04016011-13.
- 806 56. Mishra, P., Bore, T., Jiang, Y., Scheuermann, A., Li, L., 2018. Dielectric spectroscopy  
807 measurements on kaolin suspensions for sediment concentration monitoring.  
808 *Measurement*. 121, 160-169.
- 809 57. Murray, A., Skene, K., Haynes, K., 2017. The circular economy: An Interdisciplinary  
810 Exploration of the Concept and Application in a Global Context. *Journal of business  
811 ethics*. 140 (3), 369-380.
- 812 58. Muszynski, M., Vitton, S., 2012. Particle shape Estimates of Uniform Sands: Visual  
813 and Automated Methods Comparison. *Journal of Materials in Civil Engineering*. 24 (2),  
814 194-206.
- 815 59. Nash, J., Sutcliffe, J., 1970. River flow forecasting through conceptual models part  
816 I—A discussion of principles. *Journal of Hydrology*. 10 (3), 282-290.
- 817 60. Nichols, G., 2009. *Sedimentology and stratigraphy*. John Wiley & Sons.
- 818 61. Park, S., Lee, B., 2004. Studies on expansion properties in mortar containing waste  
819 glass and fibers. *Cement and concrete research*. 34 (7), 1145-1152.
- 820 62. Patel, & Vashi. 2015. *Characterization and treatment of textile wastewater*. Elsevier.
- 821 63. Peduzzi, P., 2014. Sand, rarer than one thinks. *Environmental Development*. 11, 208-  
822 218.
- 823 64. Peng, C., Scorpio, D., Kibert, C., 1997. Strategies for successful construction and  
824 demolition waste recycling operations. *Construction Management & Economics*, 15  
825 (1), 49-58.
- 826 65. Pickin, J., Randell, P., Trinh, J., Grant, B., 2018. *National Waste Report 2018*.  
827 Retrieved from:  
828 [https://www.environment.gov.au/system/files/resources/7381c1de-31d0-429b-912c-  
829 91a6dbc83af7/files/national-waste-report-2018.pdf](https://www.environment.gov.au/system/files/resources/7381c1de-31d0-429b-912c-91a6dbc83af7/files/national-waste-report-2018.pdf)
- 830 66. Qing-bing, L., XIANG, W., Lehane, B., 2011. Experimental study of effect of particle  
831 shapes on shear strength of sand and tip resistance of driven piles. *Chinese Journal of  
832 Rock Mechanics and Engineering*. 30 (2), 400-410.
- 833 67. Rashad, A., 2014. Recycled waste glass as fine aggregate replacement in cementitious  
834 materials based on Portland cement. *Construction and Building Materials*. 72, 340-357.
- 835 68. Russell, R., Taylor, R., 1937. Roundness and shape of Mississippi River sands. *The  
836 Journal of Geology*. 45 (3), 225-267.
- 837 69. Scott, B., Safiuddin, M., 2015. Abrasion resistance of concrete—design, construction  
838 and case study. *Concrete Research Letters*. 6 (3), 136-148.
- 839 70. Salamatpoor, S., Salamatpoor, S., 2017. Evaluation of adding crushed glass to different  
840 combinations of cement-stabilized sand. *International Journal of Geo-Engineering*. 8  
841 (1), 8.
- 842 71. Santamarina, J., Cho, G., 2015. Soil behaviour: The role of particle shape. *Advances in  
843 geotechnical engineering: The skempton conference*.
- 844 72. Shinohara, K., Oida, M., Golman, B., 2000. Effect of particle shape on angle of internal  
845 friction by triaxial compression test. *Powder technology*. 107 (1-2), 131-136.
- 846 73. Shishkin, A., Baronins, J., Mironovs, V., Lukáč, F., Štubňa, Igor., Ozolins, J., 2020.  
847 *Influence of Glass Additions on Illitic Clay Ceramics*. *Materials*. 13 (3), 596.

- 848 74. So, S., Lee, R., Hui, T., Shiu, Y., 2016. Study of using recycled glass cullet as an  
849 engineering fill in reclamation and earthworks in Hong Kong. Japanese Geotechnical  
850 Society Special Publication. 2 (54), 1874-1879.
- 851 75. Stahel, W., 2016. The circular economy. *Nature*. 531 (7595), 435-438.
- 852 76. Sukumaran, B., Ashmawy, A., 2001. Quantitative characterisation of the geometry of  
853 discret particles. *Geotechnique*. 51 (7), 619-627.
- 854 77. Uthus, L., Hoff, I., Horvli, I., 2019. Evaluation of grain shape characterization methods  
855 for unbound aggregates. *Proceedings of the International Conferences on the Bearing  
856 Capacity of Roads, Railways, and Airfields*.
- 857 78. Vallejo, L., Zhou, Y., 1995. The relationship between the fractal dimension and  
858 Krumbein's roundness number. *Soils and Foundations*. 35 (1), 163-167.
- 859 79. Vining, J., Linn, N., Burdge, R., 1992. Why recycle? A comparison of recycling  
860 motivations in four communities. *Environmental management*. 16 (6), 785-797.
- 861 80. WACA. 2018. What can be done about West Africa's Disappearing Sand? World Bank  
862 Group. Retrieved from:  
863 [http://documents1.worldbank.org/curated/en/501101527764779933/pdf/KS-What-](http://documents1.worldbank.org/curated/en/501101527764779933/pdf/KS-What-can-be-done-about-West-Africas-disappearing-sand.pdf)  
864 [can-be-done-about-West-Africas-disappearing-sand.pdf](http://documents1.worldbank.org/curated/en/501101527764779933/pdf/KS-What-can-be-done-about-West-Africas-disappearing-sand.pdf)
- 865 81. Wadell, H., 1932. Volume, shape, and roundness of rock particles. *The Journal of  
866 Geology*, 40 (5), 443-451.
- 867 82. Wartman, J., Grubb, D., Nasim, A., 2004. Select engineering characteristics of crushed  
868 glass. *Journal of Materials in Civil Engineering*. 16 (6), 526-539.
- 869 83. Wettimuny, R., Penumadu, D., 2004. Application of Fourier analysis to digital imaging  
870 for particle shape analysis. *Journal of Computing in Civil Engineering*. 18 (1), 2-9.
- 871 84. Woodford, C., 2019. Recycling. Retrieved from  
872 <https://www.explainthatstuff.com/recycling.html>
- 873 85. Wu, Y., Parker, F., Kandhal, P., 1998. Aggregate toughness/abrasion resistance and  
874 durability/soundness tests related to asphalt concrete performance in pavements.  
875 *Transportation Research Record*. 1638 (1), 85-93.
- 876 86. Xu, Y., Wu, S., Williams, D., Serati, M., 2018a. Determination of peak and ultimate  
877 shear strength parameters of compacted clay. *Engineering Geology*. 243, 160-167.
- 878 87. Xu, Y., Methiwala, J., Williams, D., Serati, M., 2018b. Strength and consolidation  
879 characteristics of clay with geotextile-encased sand column. *Proceedings of the  
880 Institution of Civil Engineers-Ground Improvement*. 171 (3), 125-134.
- 881 88. Xu, Y., Williams, D., Serati, M., Vangness, T., 2018. Effects of scalping on direct  
882 shear strength of crusher run and crusher run/geogrid interface. *Journal of Materials in  
883 Civil Engineering*. 30 (9), 0401820611-12.
- 884 89. Zhao, S., Zhou, X., Liu, W., 2015. Discrete element simulations of direct shear tests  
885 with particle angularity effect. *Granular Matter*. 17 (6), 793-806.
- 886 90. Zheng, J., Hryciw, R., 2016. Roundness and sphericity of soil particles in assemblies  
887 by computational geometry. *Journal of Computing in Civil Engineering*. 30 (6),  
888 04016021-13.
- 889 91. Zukri, A., Nazir, R., 2018. Sustainable materials used as stone column filler: A short  
890 review. *Materials Science and Engineering*. 342 (1), 012001.

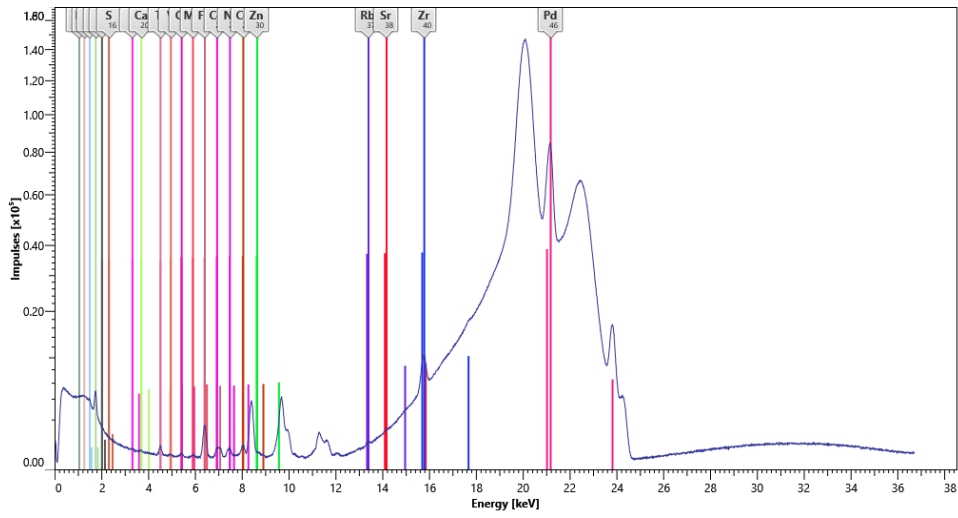
891

892

893

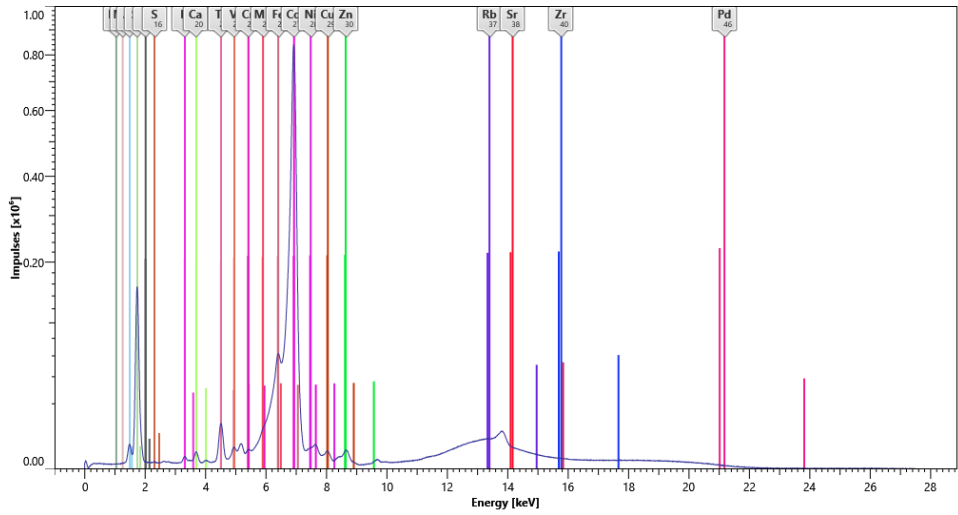
894

895 **Appendix**



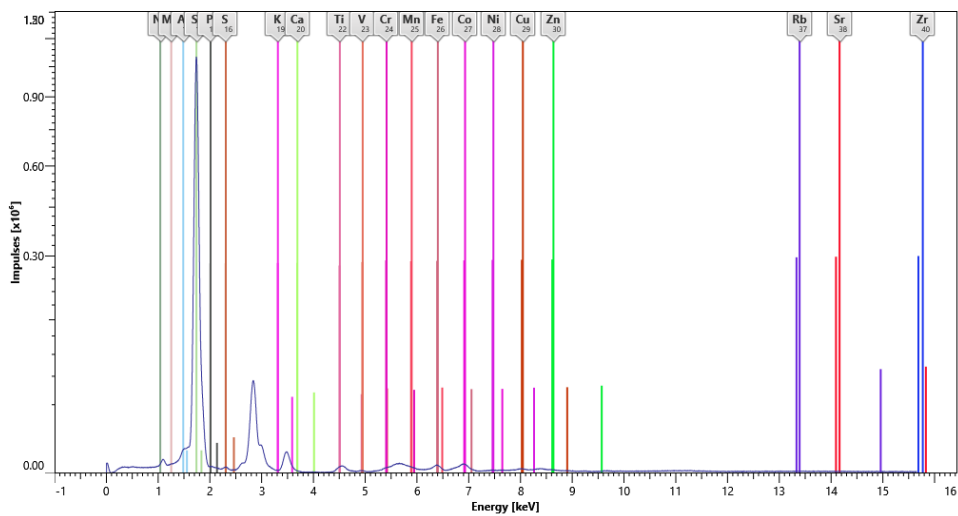
896  
897

(a)



898  
899

(b)

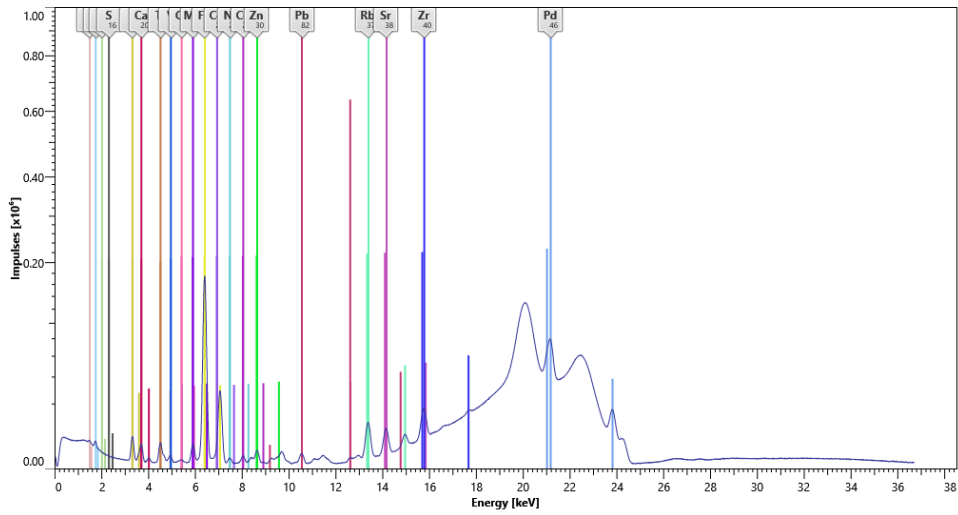


900  
901  
902

(c)

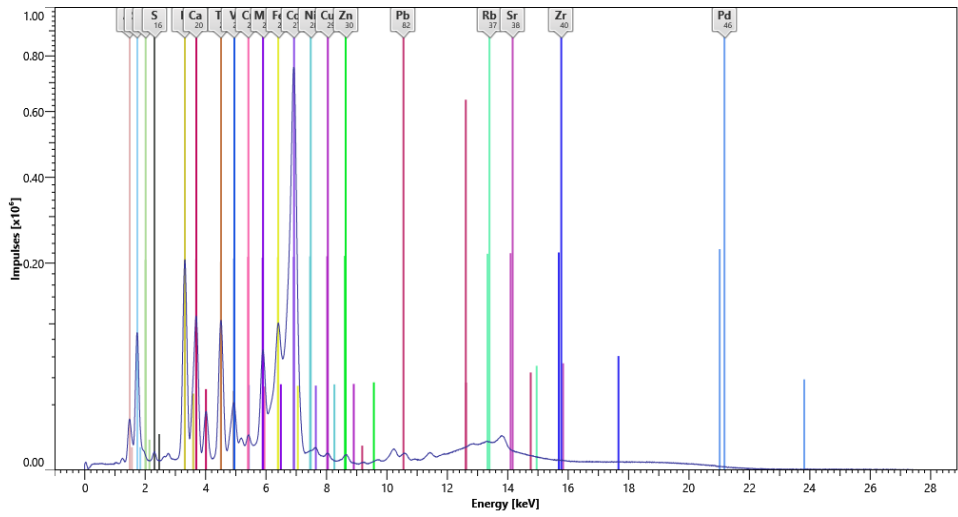
**Fig. A.1 XRF spectra of NS**





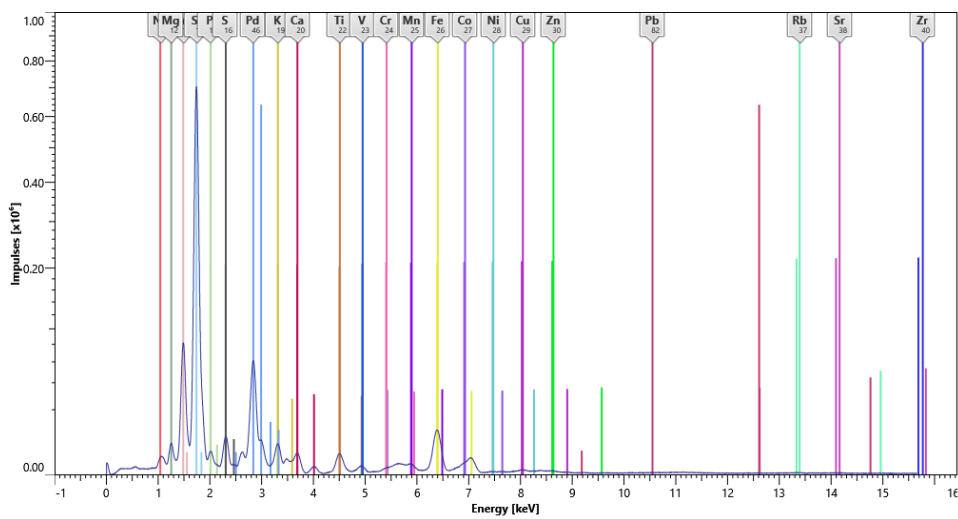
903  
904

(a)



905  
906

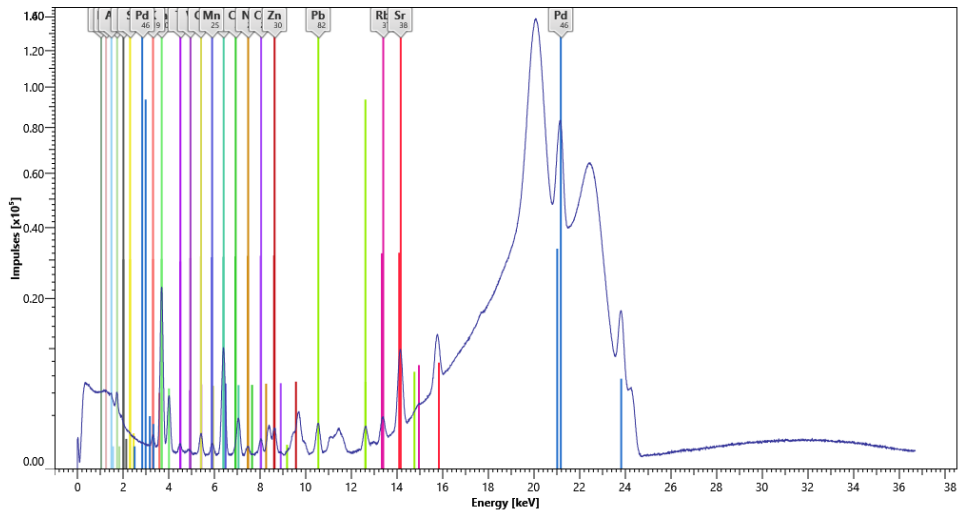
(b)



907  
908  
909

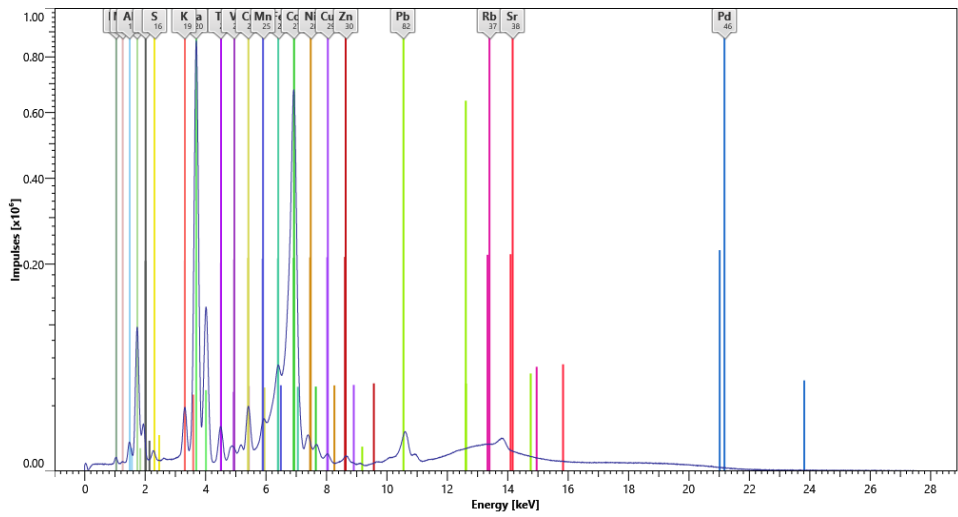
(c)

**Fig. A.2** XRF spectra of MS



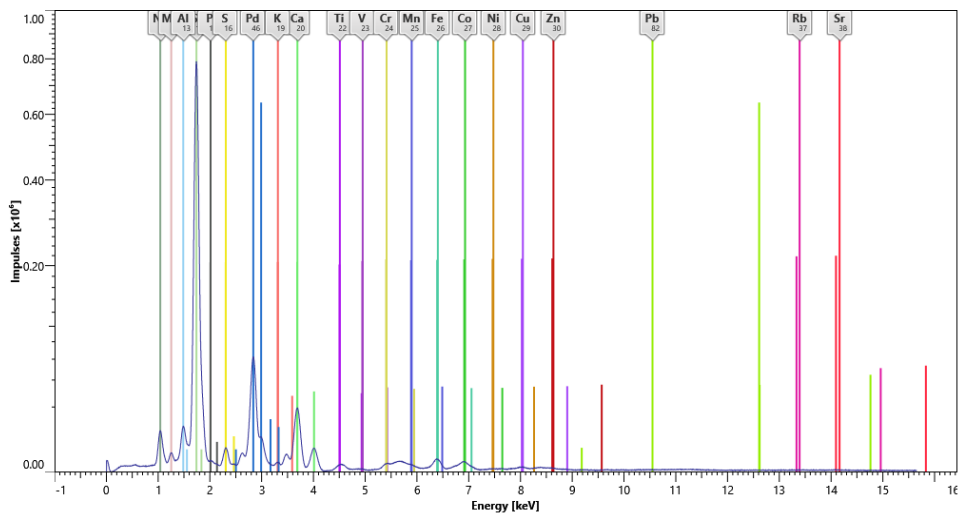
910  
911

(a)



912  
913

(b)



914  
915  
916  
917

(c)

**Fig. A.3** XRF spectra of CWG